A class of 5D Hamiltonian conservative hyperchaotic systems with symmetry and multistability

A class of 5D Hamiltonian conservative hyperchaotic systems with symmetry and multistability

Qing Dong[1], Shihua Zhou[1*], Qiang Zhang[1,2*] and Nikola K. Kasabov[3,4,5]

[1]Key Laboratory of Advanced Design and Intelligent Computing, Ministry of Education, School of Software Engineering, Dalian University, Dalian, 116622, People's Republic of China.

[2]School of Computer Science and Technology, Dalian University of Technology, Dalian, 116024, People's Republic of China.

[3]Knowledge Engineering and Discovery Research Institute, Auckland University of Technology, Auckland, 1010, New Zealand.

[4]Intelligent Systems Research Center, Ulster University, Londonderry, BT52 1SA, UK.

[5]Auckland Bioengineering Institute (ABI), The University of Auckland, Auckland, 1010, New Zealand.

*Corresponding author(s). E-mail(s): zhoushihua@dlu.edu.cn; zhangq@dlu.edu.cn;
Contributing authors: dongqing@s.dlu.edu.cn; nkasabov@aut.ac.nz;

Abstract

Conservative chaos systems have been investigated owing to their special advantages. Taking symmetry as a starting point, this study proposes a class of five-dimensional(5D) conservative hyperchaotic systems by constructing a generalized Hamiltonian conservative system. The proposed systems can have different types of coordinate-transformation and time-reversal symmetries. Also, the constructed systems are conservative in both volume and energy. The constructed systems are analyzed, and their conservative and chaotic properties are verified by relevant analysis methods, including the equilibrium points, phase diagram, Lyapunov exponent diagram, bifurcation diagram, and two-parameter Lyapunov exponent diagram. An interesting phenomenon, namely, that the proposed systems have multistable features when the initial values are changed, is observed. Furthermore, a detailed multistable characteristic analysis of two systems is performed, and it is found that the two systems have different numbers of coexisting orbits under the same energy. And, this type of system can also exhibit the coexistence of infinite orbits of different energies. Finally, the National Institute of Standards and Technology tests confirmed that the proposed systems can produce sequences with strong pseudo-randomness, and the simulation circuit is built in Multisim software to verify the simulation results of some dynamic characteristics of the system.

Keywords: Hamiltonian conservative hyperchaotic system, time-reversal symmetry, equal-energy coexisting orbit, extreme multistability

1 Introduction

Recently, many chaos systems have been reported [1–4], studied [5–7], and applied [8–10]. In the process of studying chaotic systems, an increasing number of complex dynamic properties have been introduced, such as hidden attractor, multistability, extreme multistability, and transient chaos [11–13]. These complex dynamics have been extensively used in many aspects [14–18].

Multistability is one of the many properties of a chaotic system [19–22], which signifies the coexistence of different orbits or attractors. When a chaotic system has infinitely many different orbits or attractors co-existing, it indicates that the chaotic system has extreme multistability [23–27]. Multistability or extreme multistability implies that a chaotic system has different states, which could toggle in the case of a changing system parameters. This feature makes a chaotic system highly flexible in practical applications.

Generally, chaos systems have two types: dissipative chaos systems and conservative chaos systems according to whether their energy is conserved [28]. There are two ways to judge whether a system is a conservative system; one is to judge the zero-sum feature of Lyapunov exponents [29], and another is to judge the size of its divergence by Liouville's theorem [30]. In recent studies, some multistability chaos systems have been reported. As for the research on dissipative chaotic systems, Bao et al. [31] reported a 5D hyperchaos system, which has multiple equilibria, multistability, and coordinate transformation symmetry. Yu et al. [32] introduced a 5D hyperchaos system with multiple equilibria. This system has multistable characteristics and coordinate transformation symmetry. The chaos system constructed by Wan et al. [33] has multiple attractors; however, this system has no symmetry. Yang et al. [34] constructed a 5D autonomous hyperchaotic system. This system has 15 coordinate transformation symmetries. As for the research on conservative chaotic systems, Wu et al. [35] designed a 5D smooth autonomous hyperchaos system, which has the coordinate transformation symmetry and time-reversal symmetry. However, the Hamiltonian energy of this system is conserved, while the volume is not conserved, and it does not exhibit the multistable property. Dong et al. [36] introduced a way to construct a 5D conservative hyperchaotic system. The constructed hyperchaotic system has multistable characteristics, and both the Hamiltonian energy and the volume are conserved; still, this system does not have symmetry. In [28], a 5D conservative hyperchaotic system with multistable characteristics, which has the coordinate transformation symmetry, was introduced. Hu et al. [37] reported a conservative chaos system with energy conservation. This system has coexisting orbits of equal energy, but it is conservative only in energy. In addition, this system has no symmetry.

In the existing literature, dissipative hyperchaotic systems have been extensively studied, and some of these hyperchaotic systems have extreme multistability and symmetry. However, research on conservative hyperchaotic systems is still insufficient. Recently, a few conservative hyperchaotic systems with multistable properties have been proposed. Still, there have been relatively fewer studies on conservative hyperchaotic symmetries and temporal antisymmetries.

To address the abovementioned shortcoming, this study takes symmetry as a starting point and constructs a class of symmetric 5D Hamiltonian conservative hyperchaotic systems (HCCSs) based on the existing method [36–38]. Through the analysis of the constructed conservative hyperchaotic system, it has been found that the proposed class of systems has the following characteristics: (1) its volume and energy are conservative; (2) the sum of Lyapunov exponents (LE_1–LE_5) of the constructed systems is zero, and two of them (LE_1, LE_2) are greater than zero, which meets the requirements of a 5D conservative hyperchaotic system; (3) the constructed systems have different coordinate transformation symmetries, and some of them have time-reversal symmetry; (4) the constructed systems all have multistable characteristics; (5) in the constructed systems, Type 2 [5D Hamiltonian conservative hyperchaotic systems with invariant system equations after the coordinate transformation of two system variables (HCCSs-2)] and Type 3 [5D Hamiltonian conservative hyperchaotic systems with invariant system equations after the coordinate transformation of three system variables (HCCSs-3)] have finite equal-energy orbits coexistence, and these orbits have symmetry. Meanwhile, there is also infinite different-energy orbits coexistence.

The remaining of this article is structured as follows. Section. 2 introduces an idea for

constructing a symmetry 5D conservative hyperchaotic system, in which features are discussed and proved. In section. 3, the symmetry and the multistable characteristic of system HCCSs-2.3 (one of Type 2) are analyzed. In section. 4, the equilibrium points and types, and the multistable characteristic of system HCCSs-3.1 (one of Type 3) are analyzed. In section. 5, NIST test are performed on systems HCCSs-2.3 and system HCCSs-3.1. In section. 6, the simulation circuit is constructed for system HCCSs-2.3 in Multisim software. Finally, Section. 7 draws some conclusions.

2 Proposed conservative hyperchaotic system

2.1 Propaedeutics

Arnold [39] proposed the famous Kolmogorov system. The generation mechanism of chaos can be studied by the Kolmogorov system [40]. The Kolmogorov system[41] can be expressed by equation (1).

$$\dot{\mathbf{x}} = J(\mathbf{x})\nabla H(\mathbf{x}) - \wedge\mathbf{x} + f, \tag{1}$$

where $\mathbf{x}$ refers to the state variable vector, $H(\mathbf{x}) : \mathbf{R}^n \to \mathbf{R}$ denotes the Hamiltonian energy; $J(\mathbf{x})$ is a skew-symmetric matrix, and it satifies $J(\mathbf{x}) = J(-\mathbf{x})$; $J(\mathbf{x})\nabla H(\mathbf{x})$, $\wedge\mathbf{x}$, and f represents the conservative, dissipation, and external-force terms, respectively.

When $\wedge\mathbf{x}$ and f in (1) do not exist, the Hamiltonian energy of system (1) is conserved. At this time, system (1) is called a generalized Hamiltonian conservative system [42]. The system formula is (2).

$$\dot{\mathbf{x}} = J(\mathbf{x})\nabla H(\mathbf{x}). \tag{2}$$

2.2 Construction process

According to (2), first, the Hamiltonian function [43] of a class of 5D conservative systems is assumed by equation (3).

$$H(y_1, y_2, y_3, y_4, y_5) = \frac{1}{2}(y_1^2+y_2^2+y_3^2+y_4^2+y_5^2). \tag{3}$$

The gradient of the Hamiltonian energy is formula (4).

$$\nabla H(\mathbf{x}) = [y_1, y_2, y_3, y_4, y_5]^T. \tag{4}$$

On the basis of [36, 38], the obliquely symmetric matrix $J(\mathbf{x})$ can be expressed by

$$J(\mathbf{x}) = \begin{bmatrix} 0 & y_1 & G_1 & G_2 & G_3 \\ -y_1 & 0 & y_3 & G_4 & G_5 \\ -G_1 & -y_3 & 0 & y_3 & G_6 \\ -G_2 & -G_4 & -y_3 & 0 & y_5 \\ -G_3 & -G_5 & -G_6 & -y_5 & 0 \end{bmatrix}, \tag{5}$$

where the elements' values on the sub-diagonal of the oblique symmetric matrix denote system variables; $G_1 = g_1(y_2, y_4, y_5)$, $G_2 = g_2(y_2, y_3, y_5)$, $G_3 = g_3(y_2, y_3, y_4)$, $G_4 = g_4(y_1, y_3, y_5)$, $G_5 = g_5(y_1, y_3, y_4)$, and $G_6 = g_6(y_1, y_2, y_4)$ are six three-variable functions, which are given by

$$\begin{aligned} g(m, s, p) =& (a_j m^j + a_{j-1}m^{j-1} + \cdots + a_1 m + d_1) \\ &+ (b_h s^h + b_{h-1}s^{h-1} + \cdots + b_1 s + d_2), \\ &+ (c_k p^k + c_{k-1}p^{k-1} + \cdots + c_1 p + d_3) \end{aligned} \tag{6}$$

where a_j, b_h, c_k, d_1, d_2, d_3 are constants,and $j, h, k \in Z^+$.

According to equation (2), (4) and (5) can be combined.Then, a 5D generalized Hamiltonian conservative system (7) can be obtained.

$$\begin{cases} \dot{y_1} =& y_1 y_2 + g_1(y_2, y_4, y_5)\cdot y_3 \\ & + g_2(y_2, y_3, y_5)\cdot y_4 + g_3(y_2, y_3, y_4)\cdot y_5, \\ \dot{y_2} =& -y_1^2 + y_3^2 + g_4(y_1, y_3, y_5)\cdot y_4 \\ & + g_5(y_1, y_3, y_4)\cdot y_5, \\ \dot{y_3} =& -g_1(y_2, y_4, y_5)\cdot y_1 - y_2 y_3 \\ & + y_3 y_4 + g_6(y_1, y_2, y_4)\cdot y_5, \\ \dot{y_4} =& -g_2(y_2, y_3, y_5)\cdot y_1 \\ & - g_4(y_1, y_3, y_5)\cdot y_2 - y_3^2 + y_5^2, \\ \dot{y_5} =& -g_3(y_2, y_3, y_4)\cdot y_1 - g_5(y_1, y_3, y_4)\cdot y_2 \\ & - g_6(y_1, y_2, y_4)\cdot y_3 - y_4 y_5. \end{cases} \tag{7}$$

Through analysis, it is found that the system (7) has four features:

(1) The volume of system (7) is conservative. This can be judged by Equation (8). Equation (8) represents the divergence of the system (7).

$$\nabla V = \sum_{i=1}^{5} \frac{\partial \dot{y_i}}{\partial y_i} = 0. \tag{8}$$

From Liouville's theorem [30], because $\nabla V = 0$. So it can be concluded that system (7) is volume-conservative.

(2) The Hamiltonian energy of system (7) is conservative. Equation (9) is the energy function derivative[44] of system (7).

$$\begin{aligned}\dot{H} &= \nabla H(\mathbf{x})^T \cdot \dot{\mathbf{x}} \\ &= \begin{bmatrix} y_1 \\ y_2 \\ y_3 \\ y_4 \\ y_5 \end{bmatrix}^T \cdot \begin{bmatrix} \dot{y_1} = & y_1 y_2 + g_1(y_2, y_4, y_5) \cdot y_3 \\ & + g_2(y_2, y_3, y_5) \cdot y_4 + g_3(y_2, y_3, y_4) \cdot y_5, \\ \dot{y_2} = & -y_1^2 + y_3^2 + g_4(y_1, y_3, y_5) \cdot y_4 \\ & + g_5(y_1, y_3, y_4) \cdot y_5, \\ \dot{y_3} = & -g_1(y_2, y_4, y_5) \cdot y_1 - y_2 y_3 \\ & + y_3 y_4 + g_6(y_1, y_2, y_4) \cdot y_5, \\ \dot{y_4} = & -g_2(y_2, y_3, y_5) \cdot y_1 \\ & - g_4(y_1, y_3, y_5) \cdot y_2 - y_3^2 + y_5^2, \\ \dot{y_5} = & -g_3(y_2, y_3, y_4) \cdot y_1 - g_5(y_1, y_3, y_4) \cdot y_2 \\ & - g_6(y_1, y_2, y_4) \cdot y_3 - y_4 y_5. \end{bmatrix} \\ &= 0. \end{aligned} \tag{9}$$

Since the derivative of the energy function of system (7) is zero, it can be concluded that system (7) is Hamiltonian energy conservative.

(3) The main diagonal elements of the Jacobian matrix of system (7) are not all zeros, but their sum is zero. The simplified expression of its Jacobian matrix is given by

$$J(\mathbf{x}) = \begin{bmatrix} y_2 & & & & \\ & 0 & & & \\ & & -y_2 + y_4 & & \\ & & & 0 & \\ & & & & -y_4 \end{bmatrix}. \tag{10}$$

(4) Taking the symmetry of a system as the starting point, appropriate three-variable functions are selected. Then, a 5D Hamiltonian conservative hyperchaotic system with different symmetries can be obtained. There are four construction steps:

Step 1: System (7) is obtained by constructing $J(\mathbf{x})$ and ∇H.

Step 2: Through the analysis of system (7), it can be concluded that system (7) does not have symmetry about the y_2 or y_4 coordinate transformation. However, system (7) can have other coordinate transformation symmetries and time-reversal symmetries. Based on the above analysis, appropriate three-variable functions are selected to construct system (7) with different coordinate transformation symmetries. The selected functions are all in the form of (6). However, to keep the hyperchaotic system simple, the following restriction is made: $j, h, k \in Z^+ \cup j, h, k \leqslant 1$.

Step 3: Set the system variables and initial values of system (7) so that system (7) generates hyperchaotic orbits. If there are no suitable parameters to generate a hyperchaotic system, the three-variable functions must be re-selected.

It should be noted that different choices for the number and type of functions can lead to HCCSs with different symmetries. In the following, three types of 5D conservative hyperchaotic systems are listed.

(a) Type 1: 5D HCCSs with invariant system equations after the coordinate transformation of a single system variable (HCCSs-1);

(b) Type 2: 5D HCCSs with invariant system equations after the coordinate transformation of two system variables (HCCSs-2);

(c) Type 3: 5D HCCSs with invariant system equations after the coordinate transformation of three system variables (HCCSs-3).

The above classification must be explained here. Type 2 often may have some of the symmetry of Type 1. Similarly, Type 3 may also have some of the symmetry of Type 1 and Type 2. To examine the rationality of the above way, nine 5D HCCSs with different symmetries are constructed by selecting appropriate variable functions; there are other subclasses of these systems. Table. 1, 2, and 3 list the 5D conservative hyperchaotic systems with different coordinate transformation symmetries.

The numerical simulation shows that the systems listed in Table. 1, 2, and 3 all have multistable characteristics, and the sum of LE_{1-5} are zero, and two of them (LE_1, LE_2) are greater than zero, which is in line with the characteristics of the 5D conservative hyperchaos. Furthermore, it has also been found that other systems exhibit other time-reversal symmetries, except for system HCCSs-3.3. Among the proposed systems, systems HCCSs-1.1, HCCSs-1.2, HCCSs-1.3, HCCSs-2.3, and HCCSs-3.2 have two time-reversal symmetries; system HCCSs-3.1 has three types of time-reversal symmetries; systems HCCSs-2.1 and HCCSs-2.2 have four time-reversal symmetries. In particular, systems HCCSs-1.2 and HCCSs-2.3 have full time-reversal symmetry $[(y_1, y_2, y_3, y_4, y_5, t) \rightarrow (-y_1, -y_2, -y_3, -y_4, -y_5, -t)]$. Systems HCCSs-2.3 and HCCSs-3.1 have obvious symmetry properties in the same type of hyperchaotic system. Therefore, in Section. 3 and Section. 4, the syste-

Table 1 Type 1: HCCSs-1.

System	Three-variable function	System of equations	Parameters	LE_{1-5}	Symmetry
HCCSs-1.1	$g_3(y_2,y_3,y_4)=a,$ $g_6(y_1,y_2,y_4)=by_4.$	$\begin{cases}\dot{y_1}=y_1y_2,\\ \dot{y_2}=-y_1^2+y_3^2+ay_5,\\ \dot{y_3}=-y_2y_3+y_3y_4+by_4y_5,\\ \dot{y_4}=-y_3^2+y_5^2,\\ \dot{y_5}=-y_4y_5-ay_2-by_3y_4.\end{cases}$	$a=5$ $b=2$	2.11 0.04 0 −0.04 −2.11	$R:(y_1,y_2,y_3,y_4,y_5)$ $\to(-y_1,y_2,y_3,y_4,y_5)$ $R:(y_1,y_2,y_3,y_4,y_5,t)$ $\to(y_1,-y_2,y_3,-y_4,y_5,-t)$ $R:(y_1,y_2,y_3,y_4,y_5,t)$ $\to(-y_1,-y_2,y_3,-y_4,y_5,-t)$
HCCSs-1.2	$g_1(y_1,y_3,y_4)=by_4,$ $g_2(y_2,y_3,y_5)=ay_2.$	$\begin{cases}\dot{y_1}=y_1y_2+ay_2y_4,\\ \dot{y_2}=-y_1^2+y_3^2+by_4y_5,\\ \dot{y_3}=-y_2y_3+y_3y_4,\\ \dot{y_4}=-y_3^2+y_5^2-ay_1y_2,\\ \dot{y_5}=-y_4y_5-by_2y_4.\end{cases}$	$a=5$ $b=5$	1.19 0.03 0 −0.03 −1.19	$R:(y_1,y_2,y_3,y_4,y_5)$ $\to(y_1,y_2,-y_3,y_4,y_5)$ $R:(y_1,y_2,y_3,y_4,y_5,t)$ $\to(-y_1,-y_2,y_3,-y_4,-y_5,-t)$ $R:(y_1,y_2,y_3,y_4,y_5,t)$ $\to(-y_1,-y_2,-y_3,-y_4,-y_5,-t)$
HCCSs-1.3	$g_1(y_2,y_3,y_4)=by_4,$ $g_2(y_2,y_3,y_5)=a.$	$\begin{cases}\dot{y_1}=y_1y_2+ay_4+by_3y_4,\\ \dot{y_2}=-y_1^2+y_3^2,\\ \dot{y_3}=-y_2y_3+y_3y_4-by_1y_4,\\ \dot{y_4}=-y_3^2+y_5^2-ay_1,\\ \dot{y_5}=-y_4y_5.\end{cases}$	$a=10$ $b=2.2$	1.64 0.05 0 −0.05 −1.64	$R:(y_1,y_2,y_3,y_4,y_5)$ $\to(y_1,y_2,y_3,y_4,-y_5)$ $R:(y_1,y_2,y_3,y_4,y_5,t)$ $\to(y_1,-y_2,y_3,-y_4,y_5,-t)$ $R:(y_1,y_2,y_3,y_4,y_5,t)$ $\to(y_1,-y_2,y_3,-y_4,-y_5,-t)$

Note: In Table 1, the initial value of HCCSs-1.1, HCCSs-1.2, and HCCSs-1.3 are all $(6,6,6,6,6)$.

Table 2 Type 2: HCCSs-2.

System	Three-variable function	System of equations	Parameters	LE_{1-5}	Symmetry
HCCSs-2.1	$g_2(y_2,y_3,y_5)=a.$	$\begin{cases}\dot{y_1}=y_1y_2+ay_4,\\ \dot{y_2}=-y_1^2+y_3^2,\\ \dot{y_3}=-y_2y_3+y_3y_4,\\ \dot{y_4}=-y_3^2+y_5^2-ay_1,\\ \dot{y_5}=-y_4y_5.\end{cases}$	$a=10$	0.43 0.02 0 −0.02 −0.43	$R:(y_1,y_2,y_3,y_4,y_5)$ $\to(y_1,y_2,-y_3,y_4,y_5)$ $R:(y_1,y_2,y_3,y_4,y_5)$ $\to(y_1,y_2,y_3,y_4,-y_5)$ $R:(y_1,y_2,y_3,y_4,y_5)$ $\to(y_1,y_2,-y_3,y_4,-y_5)$ $R:(y_1,y_2,y_3,y_4,y_5,t)$ $\to(y_1,-y_2,y_3,-y_4,y_5,-t)$ $R:(y_1,y_2,y_3,y_4,y_5,t)$ $\to(y_1,-y_2,-y_3,-y_4,y_5,-t)$ $R:(y_1,y_2,y_3,y_4,y_5,t)$ $\to(y_1,-y_2,y_3,-y_4,-y_5,-t)$ $R:(y_1,y_2,y_3,y_4,y_5,t)$ $\to(y_1,-y_2,-y_3,-y_4,-y_5,-t)$
HCCSs-2.2	$g_5(y_1,y_3,y_4)=a.$	$\begin{cases}\dot{y_1}=y_1y_2,\\ \dot{y_2}=-y_1^2+y_3^2+ay_5,\\ \dot{y_3}=-y_2y_3+y_3y_4,\\ \dot{y_4}=-y_3^2+y_5^2,\\ \dot{y_5}=-y_4y_5-ay_2.\end{cases}$	$a=7$	0.63 0.02 0 −0.02 −0.63	$R:(y_1,y_2,y_3,y_4,y_5)$ $\to(-y_1,y_2,y_3,y_4,y_5)$ $R:(y_1,y_2,y_3,y_4,y_5)$ $\to(y_1,y_2,-y_3,y_4,y_5)$ $R:(y_1,y_2,y_3,y_4,y_5)$ $\to(-y_1,y_2,-y_3,y_4,y_5)$ $R:(y_1,y_2,y_3,y_4,y_5,t)$ $\to(y_1,-y_2,y_3,-y_4,y_5,-t)$ $R:(y_1,y_2,y_3,y_4,y_5,t)$ $\to(y_1,-y_2,-y_3,-y_4,y_5,-t)$ $R:(y_1,y_2,y_3,y_4,y_5,t)$ $\to(-y_1,-y_2,y_3,-y_4,y_5,-t)$ $R:(y_1,y_2,y_3,y_4,y_5,t)$ $\to(-y_1,-y_2,-y_3,-y_4,y_5,-t)$
HCCSs-2.3	$g_1(y_2,y_3,y_4)=ay_5,$ $g_6(y_1,y_2,y_4)=by_1.$	$\begin{cases}\dot{y_1}=y_1y_2+ay_3y_5,\\ \dot{y_2}=-y_1^2+y_3^2,\\ \dot{y_3}=-y_2y_3+y_3y_4+(b-a)y_1y_5,\\ \dot{y_4}=-y_3^2+y_5^2,\\ \dot{y_5}=-y_4y_5-by_1y_3.\end{cases}$	$a=2$ $b=2$	0.45 0.01 0 −0.01 −0.45	$R:(y_1,y_2,y_3,y_4,y_5)$ $\to(-y_1,y_2,-y_3,y_4,y_5)$ $R:(y_1,y_2,y_3,y_4,y_5)$ $\to(y_1,y_2,-y_3,y_4,-y_5)$ $R:(y_1,y_2,y_3,y_4,y_5)$ $\to(-y_1,y_2,y_3,y_4,-y_5)$ $R:(y_1,y_2,y_3,y_4,y_5,t)$ $\to(y_1,-y_2,-y_3,-y_4,y_5,-t)$ $R:(y_1,y_2,y_3,y_4,y_5,t)$ $\to(-y_1,-y_2,-y_3,-y_4,-y_5,-t)$

Note: In Table 2, the initial value of HCCSs-2.1, HCCSs-2.2, and HCCSs-2.3 are $(2,2,10,2,2)$, $(2,2,10,2,2)$, $(-6,6,6,-6,6)$.

Table 3 Type 3: HCCSs-3.

System	Three-variable function	System of equations	Parameters	LE_{1-5}	Symmetry
HCCSs-3.1	$g_3(y_2, y_3, y_4) = a.$	$\begin{cases} \dot{y_1} = y_1y_2 + ay_5, \\ \dot{y_2} = -y_1^2 + y_3^2, \\ \dot{y_3} = -y_2y_3 + y_3y_4, \\ \dot{y_4} = -y_3^2 + y_5^2, \\ \dot{y_5} = -y_4y_5 - ay_1. \end{cases}$	$a = 5$	$\begin{matrix} 0.36 \\ 0.01 \\ 0 \\ -0.01 \\ -0.36 \end{matrix}$	$\begin{matrix} R : (y_1, y_2, y_3, y_4, y_5) \\ \to (y_1, y_2, -y_3, y_4, y_5) \\ R : (y_1, y_2, y_3, y_4, y_5) \\ \to (-y_1, y_2, y_3, y_4, -y_5) \\ R : (y_1, y_2, y_3, y_4, y_5) \\ \to (-y_1, y_2, -y_3, y_4, -y_5) \\ R : (y_1, y_2, y_3, y_4, y_5, t) \\ \to (y_1, -y_2, y_3, -y_4, -y_5, -t) \\ R : (y_1, y_2, y_3, y_4, y_5, t) \\ \to (-y_1, -y_2, -y_3, -y_4, y_5, -t) \\ R : (y_1, y_2, y_3, y_4, y_5, t) \\ \to (y_1, -y_2, -y_3, -y_4, -y_5, -t) \end{matrix}$
HCCSs-3.2	$g_3(y_2, y_3, y_4) = a,$ $g_6(y_1, y_2, y_3) = b.$	$\begin{cases} \dot{y_1} = y_1y_2 + ay_3, \\ \dot{y_2} = -y_1^2 + y_3^2, \\ \dot{y_3} = -y_2y_3 + y_3y_4 - ay_1 + by_5, \\ \dot{y_4} = -y_3^2 + y_5^2, \\ \dot{y_5} = -y_4y_5 - by_3. \end{cases}$	$a = 10$ $b = 10$	$\begin{matrix} 0.43 \\ 0.01 \\ 0 \\ -0.01 \\ -0.43 \end{matrix}$	$\begin{matrix} R : (y_1, y_2, y_3, y_4, y_5) \\ \to (-y_1, y_2, -y_3, y_4, -y_5) \\ R : (y_1, y_2, y_3, y_4, y_5, t) \\ \to (y_1, -y_2, -y_3, -y_4, y_5, -t) \\ R : (y_1, y_2, y_3, y_4, y_5, t) \\ \to (-y_1, -y_2, y_3, -y_4, -y_5, -t) \end{matrix}$
HCCSs-3.3	$g_3(y_2, y_3, y_4) = a,$ $g_4(y_1, y_3, y_5) = c,$ $g_6(y_1, y_2, y_3) = b.$	$\begin{cases} \dot{y_1} = y_1y_2 + ay_3, \\ \dot{y_2} = -y_1^2 + y_3^2 + cy_4, \\ \dot{y_3} = -y_2y_3 + y_3y_4 - ay_1 + by_5, \\ \dot{y_4} = -y_3^2 + y_5^2 - cy_2, \\ \dot{y_5} = -y_4y_5 - by_3. \end{cases}$	$a = 10$ $b = 13$ $c = 10$	$\begin{matrix} 1.18 \\ 0.02 \\ 0 \\ -0.02 \\ -1.18 \end{matrix}$	$\begin{matrix} R : (y_1, y_2, y_3, y_4, y_5) \\ \to (-y_1, y_2, -y_3, y_4, -y_5) \end{matrix}$

Note: In Table 3, the initial value of HCCSs-3.1, HCCSs-3.2, and HCCSs-3.3 are $(6, -6, 6, 6, 6)$, $(-6, 6, -6, 6, 6)$, $(6, 6, 6, 6, 6)$.

ms HCCSs-2.3 and HCCSs-3.1 were analyzed as examples.

3 Dynamics analysis of HCCSs-2.3

In this section, system HCCSs-2.3 is analyzed as a representative of Type 2 systems, namely, HCCSs-2 systems. The system equations of system HCCSs-2.3 are given by

$$\begin{cases} \dot{y_1} = y_1y_2 + ay_3y_5, \\ \dot{y_2} = -y_1^2 + y_3^2, \\ \dot{y_3} = -y_2y_3 + y_3y_4 + (b-a)y_1y_5, \\ \dot{y_4} = -y_3^2 + y_5^2, \\ \dot{y_5} = -y_4y_5 - by_1y_3. \end{cases} \tag{11}$$

The parameters of system HCCSs-2.3 are selected using $(a, b) = (2, 2)$, and their initial values are $(y_{10}, y_{20}, y_{30}, y_{40}, y_{50}) = (-6, 6, 6, -6, 6)$. Then, the computed results of (LE_1–LE_5) are: 0.45, 0.01, 0, −0.01, −0.45, and the sum of LE_1–LE_5 is zero. In addition, the Lyapunov dimension is got by equation (12).

$$\begin{aligned} D &= 4 + \frac{LE_1 + LE_2 + LE_3 + LE_4}{|LE_5|} \\ &= 4 + \frac{0.45 + 0.01 + 0 - 0.01}{|-0.45|} \\ &= 5. \end{aligned} \tag{12}$$

It can be seen that the Kaplan-Yorke dimension of HCCSs-2.3 is equal to the system dimension. This also confirms the conservatism of the system from another aspect. Next, we investigate the dynamics of the system using different methods.

3.1 Coordinate-transformation and time-reversal symmetry

When the sign of one or more state variables of the system changes, and the changed system is equivalent to the original system, it means that the system has coordinate transformation symmetry. Time-reversal symmetry[7, 45] indicates that under the time transformation $t \to -t$, the sign of one or multiple state variables of the system changes, but the transformed system is equivalent to the original system. A special transformation in time-reversal symmetry is full time-reversal symmetry, which means that under the time transformation $t \to -t$, the signs of all state variables change, but the transformed system is equivalent to the original system. Time-reversal symmetry has been common in conservative systems but less common in dissipative systems [46]. Time-reversal symmetry is crucial in analyzing many physical models [47, 48].

System HCCSs-2.3 has the three following coordinate transformation symmetries: R : $(y_1, y_2, y_3, y_4, y_5) \rightarrow (-y_1, y_2, -y_3, y_4, y_5)$, R : $(y_1, y_2, y_3, y_4, y_5) \rightarrow (y_1, y_2, -y_3, y_4, -y_5)$, R : $(y_1, y_2, y_3, y_4, y_5) \rightarrow (-y_1, y_2, y_3, y_4, -y_5)$. Also, it has partial and full time-reversal symmetry.

First, the coordinate transformation symmetry of $R : (y_1, y_2, y_3, y_4, y_5, t) \rightarrow (y_1, -y_2, -y_3, -y_4, y_5, -t)$ is used to obtain the following expressions:

$$\begin{cases} \frac{-dy_1}{dt} = y_1(-y_2) + a(-y_3)y_5, \\ \frac{-dy_2}{-dt} = -y_1^2 + (-y_3)^2, \\ \frac{-dy_3}{-dt} = -y_2y_3 + y_3y_4 + (b-a)y_1y_5, \\ \frac{-dy_4}{-dt} = -(-y_3)^2 + y_5^2, \\ \frac{-dy_5}{dt} = -y_5(-y_4) - by_1(-y_3). \end{cases} \tag{13}$$

Then, the coordinate transformation symmetry of $R : (y_1, y_2, y_3, y_4, y_5, t) \rightarrow (-y_1, -y_2, -y_3, -y_4, -y_5, -t)$ is used to obtain the following expressions:

$$\begin{cases} \frac{-dx}{-dt} = y_1y_2 + ay_3y_4, \\ \frac{-dy}{-dt} = -y_1^2 + y_3^2, \\ \frac{-dz}{-dt} = -y_2y_3 + y_3y_4 + (b-a)y_1y_5, \\ \frac{-dw}{-dt} = -y_3^2 + y_5^2, \\ \frac{-du}{-dt} = -y_4y_5 - by_1y_3. \end{cases} \tag{14}$$

The systems (11), (13), and (14) are the same, indicating that the system HCCSs-2.3 has partial time-reversal symmetry and full time-reversal symmetry. Among the 5D conservative hyperchaotic systems proposed to date [28, 35, 36], there has been no system with both partial time-reversal symmetry and full time-reversal symmetry. This property is the first to be found in a 5D conservative hyperchaotic system.

3.2 Equilibrium points

In this subsection, the equilibrium point of the system HCCSs-2.3 is analyzed.

Firstly, let each expression in the equation (11) be equal to zero, equation(15) can be obtained:

$$\begin{cases} y_1y_2 + ay_3y_5 = 0, \\ -y_1^2 + y_3^2 = 0, \\ -y_2y_3 + y_3y_4 + (b-a)y_1y_5 = 0, \\ -y_3^2 + y_5^2 = 0, \\ -y_4y_5 - by_1y_3 = 0. \end{cases} \tag{15}$$

It is easy to obtain the equilibrium point of the system HCCSs-2.3 as ($|l|$,$-a|l|$,$|l|$,$-b|l|$,$|l|$), where $l \in R$.

Then, its Jacobian matrix is calculated by the system equation (11). The Jacobian matrix of system HCCSs-3.1 is given by

$$J_2(\mathbf{x}) = \begin{bmatrix} y_2 & y_1 & ay_5 & 0 & ay_3 \\ -2y_1 & 0 & 2y_3 & 0 & 0 \\ (b-a)y_5 & -y_3 & -y_2+y_4 & y_3 & (b-a)y_1 \\ 0 & 0 & -2y_3 & 0 & 2y_5 \\ -by_3 & 0 & -by_1 & -y_5 & -y_4 \end{bmatrix}. \tag{16}$$

Next, bringing the equilibrium points ($|l|$,$-a|l|$,$|l|$,$-b|l|$,$|l|$) into the formula (16), the characteristic polynomial (17) can be obtained.

$$f(\lambda) = \lambda[\lambda^4 + 24y_1^3\lambda^2 + 44y_1^4]. \tag{17}$$

The above calculation process needs to be explained here. Since the equilibrium point contains absolute values, this equilibrium point has many forms (8 types in total), that is, the system has eight plane equilibrium points. Through calculation, it is found that these equilibrium points have the same characteristic polynomial (17).

Let the characteristic polynomial (17) be zero; then, the characteristic values $(0, \eta, -\eta, j\varphi, -j\varphi)$, $(0, j\varphi_1, -j\varphi_1, j\varphi_2, -j\varphi_2)$, $(0, \eta + j\varphi_1, \eta - j\varphi_1, -\eta + j\varphi_2, -\eta - j\varphi_2)$ can be obtained, where $(\eta, \varphi > 0)$. Then, according to the calculated eigenvalues, it can be determined that the corresponding equilibrium point types are saddle point, center point, and saddle point. This is consistent with the characteristics of conservative chaotic systems.

3.3 Effect of parameter a on system HCCSs-2.3 performance

The nature of a chaos system is correlated with the adjustable parameter. In this subsection, we mainly discuss the influence on system HCCSs-2.3 performance when adjustable parameter a changes.

Set the initial value and adjustable parameter be $(-6,\ 6,\ 6,\ -6,\ 6)$ and $a \in [0, 500]$, respectively. The Lyapunov exponent diagram of system HCCSs-2.3 can be obtained, as shown in Fig. 1a. To more clearly reflect the nature of the system, a bifurcation diagram of the same range was also made, as shown in Fig. 1b. As can be observed, they reflect the same dynamic behavior.

By observing Fig. 1, it can be found that the system HCCSs-2.3 has been in a hyperchaotic

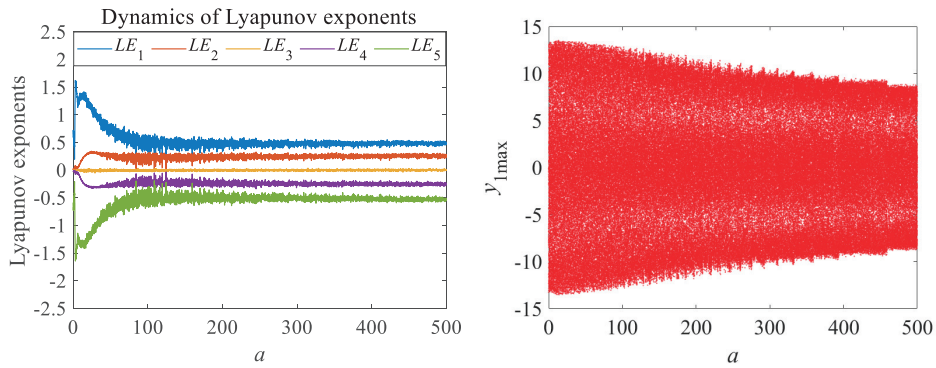

Fig. 1 System HCCSs-2.3. **a** The Lyapunov exponent diagram when a changes; **b** the corresponding bifurcation diagram.

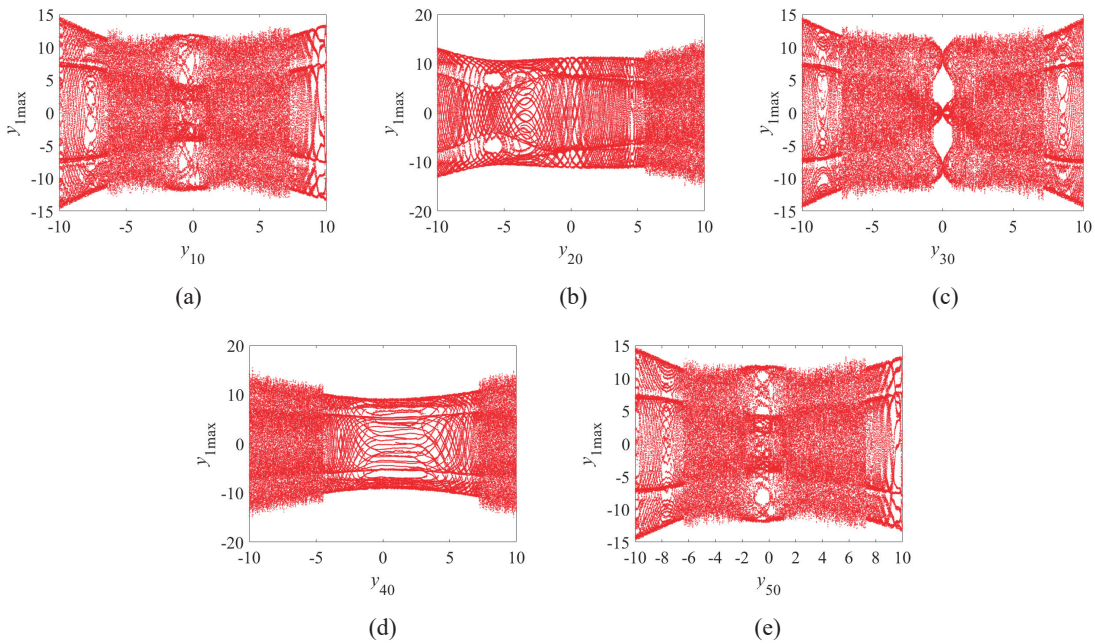

Fig. 2 The bifurcation diagrams of the system HCCSs-2.3 for different initial parametres. **a** $y_{10} \in [-10, 10]$; **b** $y_{20} \in [-10, 10]$; **c** $y_{30} \in [-10, 10]$; **d** $y_{40} \in [-10, 10]$; **e** $y_{50} \in [-10, 10]$.

state in the range of $a \in [0, 500]$. This shows that the system can remain chaotic in a wide range of parameters without generating other states (periodic or quasi-periodic). Under such parameters, the system is more stable.

3.4 Bifurcation diagram of HCCSs-2.3

Set parameters to $(a, b) = (2, 2)$, then change the initial values of the system parameters y_{10}, y_{20}, y_{30}, y_{40}, and y_{50}. Make the initial value the following values, $(y_{10}, 6, 6, -6, 6)$, $(-6, y_{20}, 6, -6, 6)$, $(-6, 6, y_{30}, -6, 6)$, $(-6, 6, 6, y_{40}, 6)$, $(-6, 6, 6, -6, y_{50})$, and $y_{10} \in [-10, 10]$, $y_{20} \in [-10, 10]$, $y_{30} \in [-10, 10]$, $y_{40} \in [-10, 10]$, $y_{50} \in [-10, 10]$. The bifurcation diagrams of HCCSs-2.3 for different initial value ranges are made, as shown in Fig. 2.

According to the differences between the bifurcation diagrams in Fig. 2, it can be found that different initial values lead to different chaotic or

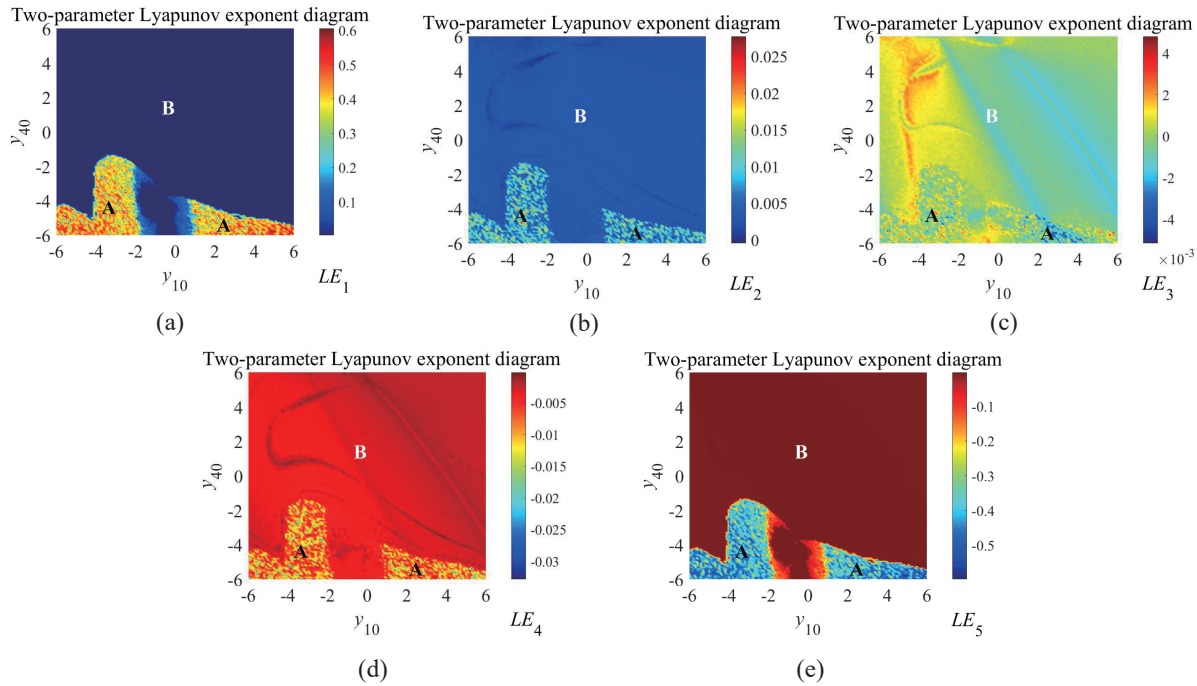

Fig. 3 Two-parameter Lyapunov exponent spectrum. **a** LE_1; **b** LE_2; **c** LE_3; **d** LE_4 ; **e** LE_5

quasi-periodic orbits. This phenomenon indicates that chaotic (hyperchaotic) orbits coexist with quasi-periodic (periodic) orbits in system HCCSs-2.3.

3.5 Two-parameter Lyapunov exponent spectrum

A useful instrument for analyzing the multistability property of chaotic systems is the two-parameter Lyapunov exponent spectrum, which is also known as the dynamic evolution graph[28]. In a dynamic evolution graph, different colors represent the Lyapunov exponent values of different sizes, which are used to illustrate system characteristics graphically.

For system HCCSs-2.3, the system parameters for $(a, b) = (2, 2)$ are determined. Its initial values are $(y_{10},\ 6,\ 6,\ y_{40},\ 6)$, where $y_{10} \in [-6, 6]$, $y_{40} \in [-6, 6]$. Therefore, five Lyapunov exponents in the above two intervals, denoted LE_1–LE_5, are obtained. The dynamic evolution diagram can clearly demonstrate the coexistence of different orbits.

The Lyapunov exponent of system HCCSs-2.3 is symmetric about the zero axis, as shown in Fig. 3. Different orbits can coexist under different initial values. This indicates that this system switches between different initial hyperchaotic (chaotic) and quasi-periodic (periodic) values, i.e., it has a multistable nature. In region A, the system HCCSs-2.3 is chaotic or hyperchaotic, since LE_1 is greater than zero and LE_2 is greater than or equal to zero. Furthermore, all Lyapunov exponents of system HCCSs-2.3 in region B are approximately zero, which indicates that system HCCSs-2.3 is quasi-periodic or periodic. The multistable state of system HCCSs-2.3 is discussed in Section. 3.6.

3.6 Multistability analysis

Multistability is a subject of importance in studying chaos[44]. In conservative chaos systems, because they have no attractors, the multistability characteristic that they possess is often called the coexistence of multiple orbits.

3.6.1 Equal-energy orbit coexistence

According to the results in Fig. 3, system HCCSs-2.3 is multistable. On this basis, by changing the sign of initial value of $(-6,\ 6,\ 6,\ -6,\ 6)$ of system HCCSs-2.3, the Hamiltonian energy of the system

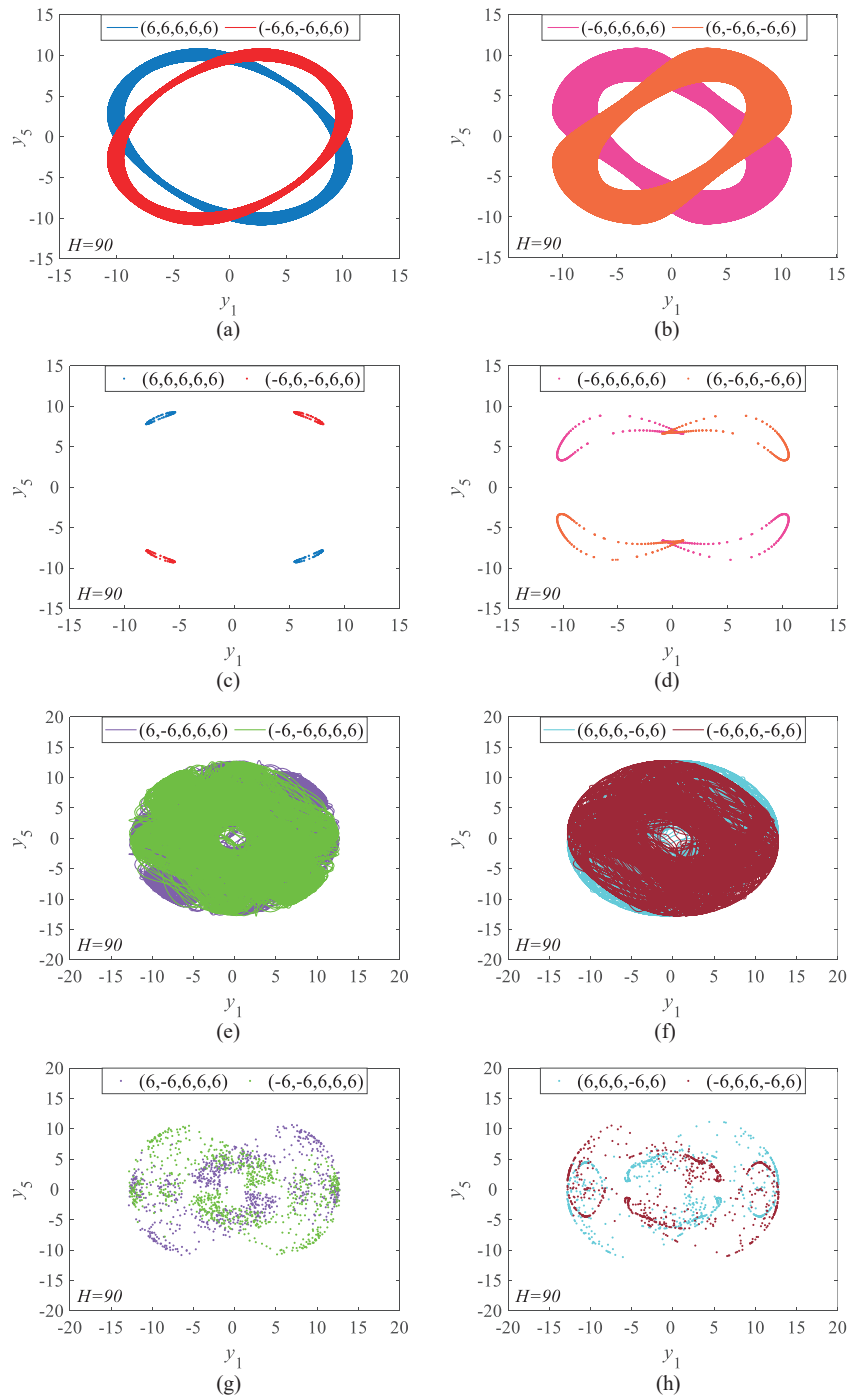

Fig. 4 The phase trajectory diagrams of system HCCSs-2.3 on the $y_1 - y_5$ plane for different initial values. **a**, **b** Coexisting quasi-periodic orbits of equal energy and symmetry; **c** Poincaré section corresponding to a; **d** Poincaré section corresponding to b; **e**, **f** coexisting chaotic orbits of equal energy and symmetry; **g** Poincaré section corresponding to e; **h** Poincaré section corresponding to f.

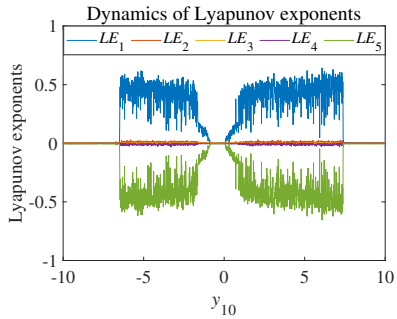

Fig. 5 Lyapunov exponent spectrum with respect to y_{10}, where $y_{10} \in [-10, 10]$

remains unchanged, that is, the Hamiltonian energy has a constant value of 90, as given by

$$H(y_{10}, y_{20}, y_{30}, y_{40}, y_{50}) = \frac{1}{2}(y_{10}^2 + y_{20}^2 + y_{30}^2 + y_{40}^2 + y_{50}^2) = 90. \tag{18}$$

Set the initial conditions of system HCCSs-2.3 to (6, 6, 6, 6, 6), (−6, 6, −6, 6, 6), (−6, 6, 6, 6, 6), (6, −6, 6, −6, 6), (−6, −6, 6, 6, 6), (6, −6, 6, 6, 6), (6, 6, 6, −6, 6), (−6, 6, 6, −6, 6) in turn. In this way, quasi-periodic and chaotic orbits with the same energy can coexist. In this case, there are eight quasi-periodic and chaotic orbits with the same energy coexisting in system HCCSs-2.3, and these orbits have symmetry. The phase trajectory diagrams in the $y_1 - y_5$ plane of system HCCSs-2.3 with eight coexisting quasi-periodic and chaotic orbits with the same energy, corresponding to certain initial values and its Poincaré sections are shown in Fig. 4. It should be noted that Fig. 4a and b correspond to the quasi-periodic orbits; Fig. 4c and d are the Poincaré sections of a and b, respectively; Fig. 4e and f correspond to chaotic orbits; Fig. 4g and 3h correspond to the Poincaré sections of e and f. The results in Fig. 4 show that system HCCSs-2.3 can produce orbits with the same Hamiltonian energy at the same time, i.e., there is a multistable state with the same Hamiltonian energy characteristic. In Fig. 4e and f, the chaotic orbits have the symmetry property in their phase trajectory diagrams and Poincaré cross-sections, but their Lyapunov exponents are not the same. This special phenomenon has also been reported in [46]. However, this system is a conservative chaotic system, not a conservative hyperchaotic system.

3.6.2 Different-energy orbit coexistence

By studying the coexistence of orbits of the same energy in the system HCCSs-2.3, it has been found that the system has coexisting orbits with different Hamiltonian energies under different initial values.

Let the system parameters be $(a, b) = (2, 2)$. Change the system initial value y_{10} such that (y_{10}, 6, 6, −6, 6), where $y_{10} \in [-10, 10]$. Fig. 5 is the Lyapunov exponent spectrum of system HCCSs-2.3. Fig. 2d is the bifurcation diagram under the same range. The Lyapunov exponent of system HCCSs-2.3 is symmetrical about the zero axis in the whole interval, which indicates the conservation of the system.

Set y_{10} in system HCCSs-2.3 to −9.88, −8.28, −6.53, −5.25, −0.53, 4.26, 7.71, 9.42, 9.9 in turn while keeping the other system parameters unchanged. The obtained phase trajectory diagrams in the $y_1 - y_5$ plane are shown in Fig. 6. The system HCCSs-2.3 has the features of coexistence of quasi-periodic, chaos(hyperchaos) orbits.

4 Dynamics analysis of system HCCSs-3.1

In this section, system HCCSs-3.1, which is a Type 3 system, is analyzed. The analysis mainly includes the equilibrium points and multistable characteristic analysis.

The system equations of system HCCSs-3.1 are given by

$$\begin{cases} \dot{y_1} = y_1 y_2 + a y_5, \\ \dot{y_2} = -y_1^2 + y_3^2, \\ \dot{y_3} = -y_2 y_3 + y_3 y_4, \\ \dot{y_4} = -y_3^2 + y_5^2, \\ \dot{y_5} = -y_4 y_5 - a y_1. \end{cases} \tag{19}$$

4.1 Equilibrium points

Let each expression in the equation (19) be equal to zero, the following expressions can be obtained:

$$\begin{cases} y_1 y_2 + a y_5 = 0, \\ -y_1^2 + y_3^2 = 0, \\ -y_2 y_3 + y_3 y_4 = 0, \\ -y_3^2 + y_5^2 = 0, \\ -y_4 y_5 - a y_1 = 0. \end{cases} \tag{20}$$

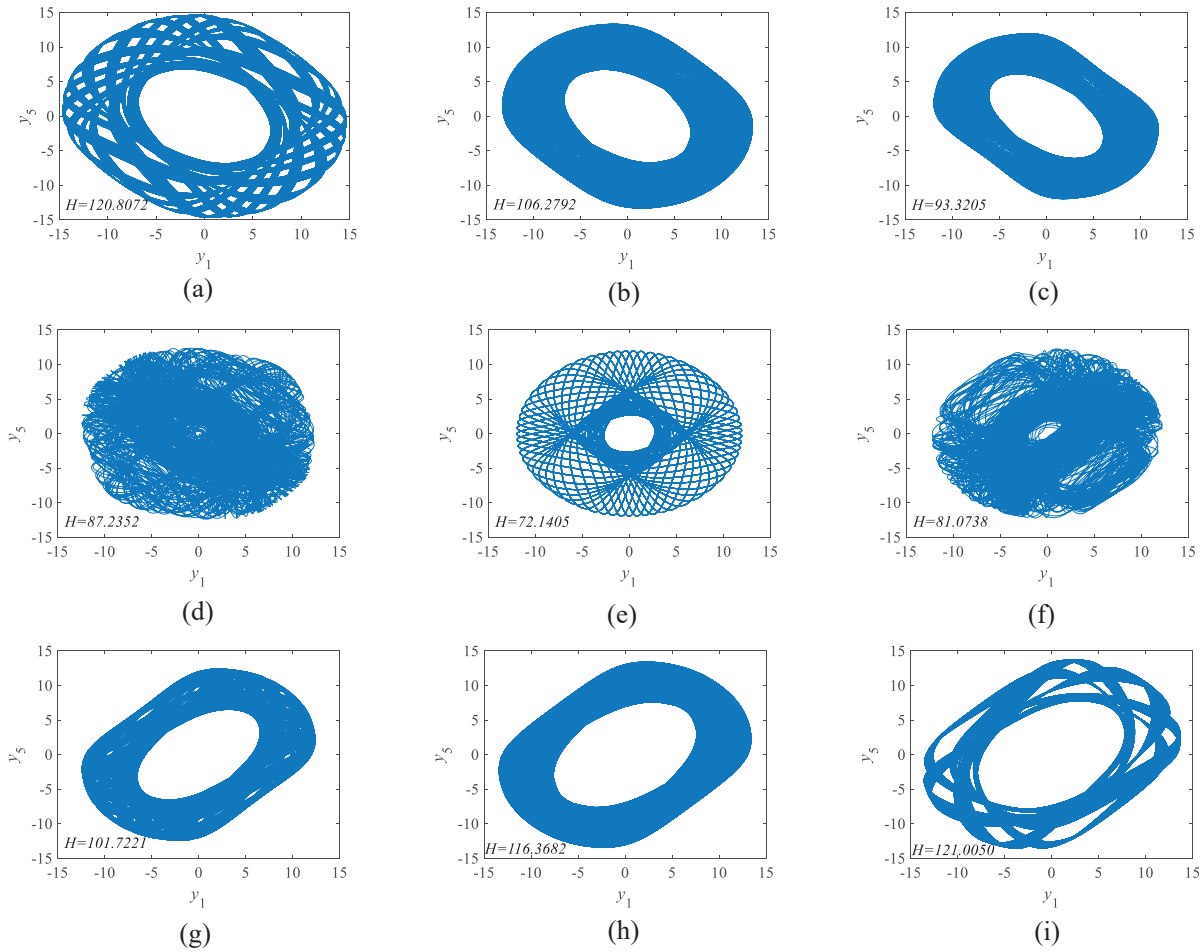

Fig. 6 Phase trajectories of the $y_1 - y_5$ plane of system HCCSs-2.3 at different initial values of y_{10}. **a** $y_{10} = -9.88$; **b** $y_{10} = -8.28$; **c** $y_{10} = -6.53$; **d** $y_{10} = -5.52$; **e** $y_{10} = -0.53$; **f** $y_{10} = 4.26$; **g** $y_{10} = 7.71$; **h** $y_{10} = 9.42$; **i** $y_{10} = 9.9$.

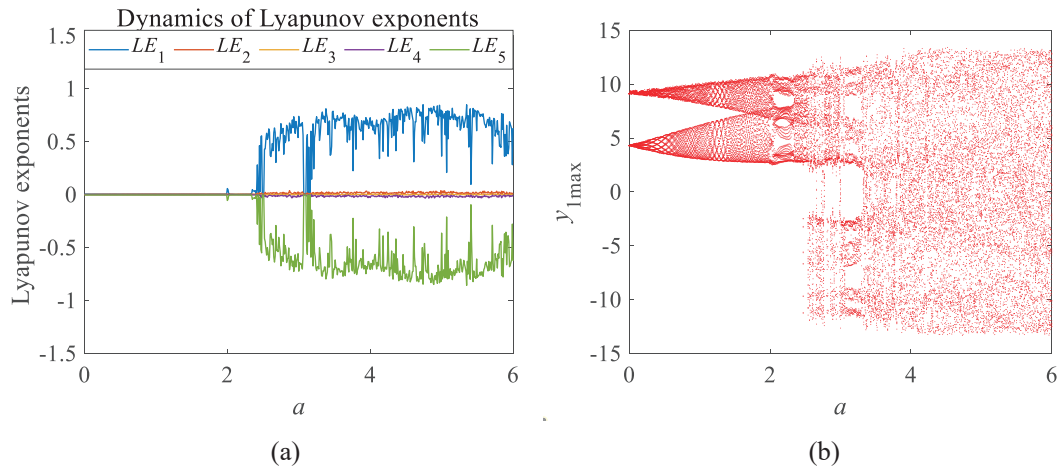

Fig. 7 System HCCSs-3.1. **a** The Lyapunov exponent diagram when a changes; **b** the corresponding bifurcation diagram.

By calculation, the equilibrium points of the system can be obtained as (0,0,0,0,0), (0,q_2,0,0,0), (0,0,0,q_4,0), (0,q_2,0,q_4,0), ($\pm q_1, \mp a, |q_1|, \mp a, \pm q_1$), where q_1, q_2, $q_4 \in R$. System HCCSs-3.1 has three line equilibrium points and two surface equilibrium points. The Jacobian matrix of system HCCSs-3.1 is given by

$$J_2(\mathbf{x}) = \begin{bmatrix} y_2 & y_1 & 0 & 0 & a \\ -2y_1 & 0 & 2y_3 & 0 & 0 \\ 0 & -y_3 & -y_2+y_4 & y_3 & 0 \\ 0 & 0 & -2y_3 & 0 & 2y_5 \\ -a & 0 & 0 & -y_5 & -y_4 \end{bmatrix}. \quad (21)$$

By importing the equilibrium points (0,0,0,0,0), (0,q_2,0,0,0), (0,0,0,q_4,0), (0,q_2,0,q_4,0), ($\pm q_1, \mp a, |q_1|, \mp a, \pm q_1$) into the Jacobian matrix (21), the corresponding characteristic polynomial can be obtained as follows:

$$f_1(\lambda) = \lambda^3(\lambda^2 + 25), \quad (22)$$

$$f_2(\lambda) = \lambda^2(\lambda^3 + (25 - y_2^2)\lambda + 25y_2), \quad (23)$$

$$f_3(\lambda) = \lambda^2(\lambda^3 + (25 - y_4^2)\lambda - 25y_4), \quad (24)$$

$$f_4(\lambda) = \lambda^2[\lambda^3 + (25 + y_2y_4 - y_2^2 - y_2^4)\lambda - (y_4 - y_2)(y_2y_4 - 25)], \quad (25)$$

$$f_5(\lambda) = \lambda(\lambda^4 + 8y_1^2\lambda^2 + 12y_1^4). \quad (26)$$

Let the characteristic polynomials (22), (23), (24), (25), and (26) be zero; then, the corresponding eigenvalues can be obtained. Then, the equilibrium point type of the system is judged according to the literature[28, 44, 49], as shown in Table. 4.

In Table. 4, the equilibrium point types of HCCSs-3.1 are only the center point and saddle point. This is consistent with the related theory in the existing literature expressing that a system with a center point or a saddle point can produce a conservative chaotic orbit [50, 51].

4.2 Effect of parameter a on system HCCSs-3.1 performance

The nature of a chaos system is correlated with the system parameters, including the adjustable parameter and initial value. Next, we mainly discuss the influence on system HCCSs-3.1 performance when adjustable parameter a changes.

Let the initial value and adjustable parameter be (6, −6, 6, 6, 6) and $a \in [0, 6]$, respectively; set the step size to 0.01. The Lyapunov exponent diagram of system HCCSs-3.1 can be obtained, as shown in Fig. 7a. To more clearly reflect the nature of the system, a bifurcation diagram of the same range was also made, as shown in Fig. 7b. As can be observed, they reflect the same dynamic behavior.

Table 4 The equilibrium points of System HCCSs-3.1 and their types.

System	Equilibrium points	Eigenvalues ($\varepsilon, \mu > 0$)	Equilibrium points type
HCCSs-3.1	(0,0,0,0,0)	$(0, 0, 0, j\mu, -j\mu)$	Center
	(0,q_2,0,0,0)	$(0, 0, 0, \varepsilon, -\varepsilon)$	Saddle
		$(0, 0, 0, j\mu, -j\mu)$	Center
		$(0, 0, -\varepsilon_1, \varepsilon_2 + j\mu_1, \varepsilon_2 - j\mu_1)$	Saddle
		$(0, 0, \varepsilon_1, -\varepsilon_2 + j\mu_1, -\varepsilon_2 - j\mu_1)$	Saddle
	(0,0,0,q_4,0)	$(0, 0, 0, \varepsilon, -\varepsilon)$	Saddle
		$(0, 0, 0, j\mu, -j\mu)$	Center
		$(0, 0, -\varepsilon_1, \varepsilon_2 + j\mu_1, \varepsilon_2 - j\mu_1)$	Saddle
		$(0, 0, \varepsilon_1, -\varepsilon_2 + j\mu_1, -\varepsilon_2 - j\mu_1)$	Saddle
	(0,q_2,0,q_4,0)	$(0, 0, 0, \varepsilon, -\varepsilon)$	Saddle
		$(0, 0, 0, j\mu, -j\mu)$	Center
		$(0, 0, -\varepsilon_1, \varepsilon_2 + j\mu_1, \varepsilon_2 - j\mu_1)$	Saddle
		$(0, 0, \varepsilon_1, -\varepsilon_2 + j\mu_1, -\varepsilon_2 - j\mu_1)$	Saddle
	($\pm q_1, \mp a, \lvert q_1\rvert, \mp a, \pm q_1$)	$(0, \varepsilon_3, -\varepsilon_3, j\mu_2, -j\mu_2)$	Saddle
		$(0, j\mu_3, -j\mu_3, j\mu_4, -j\mu_4)$	Center
		$(0, \varepsilon_3 + j\mu_3, \varepsilon_3 - j\mu_3, -\varepsilon_3 + j\mu_4, -\varepsilon_3 - j\mu_4)$	Saddle

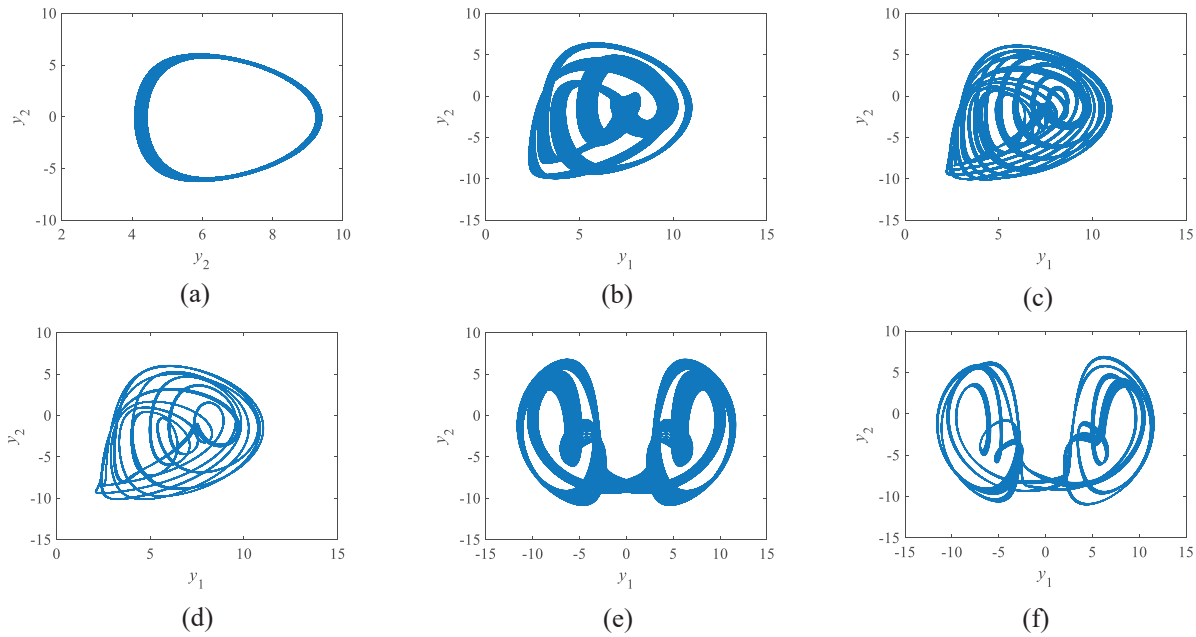

Fig. 8 The phase trajectories of the system on the $y_1 - y_2$ plane. **a** a=0.1; **b** a=2.15; **c** a=2.43; **d** a=2.50; **e** a=3.09; **f** a=3.15.

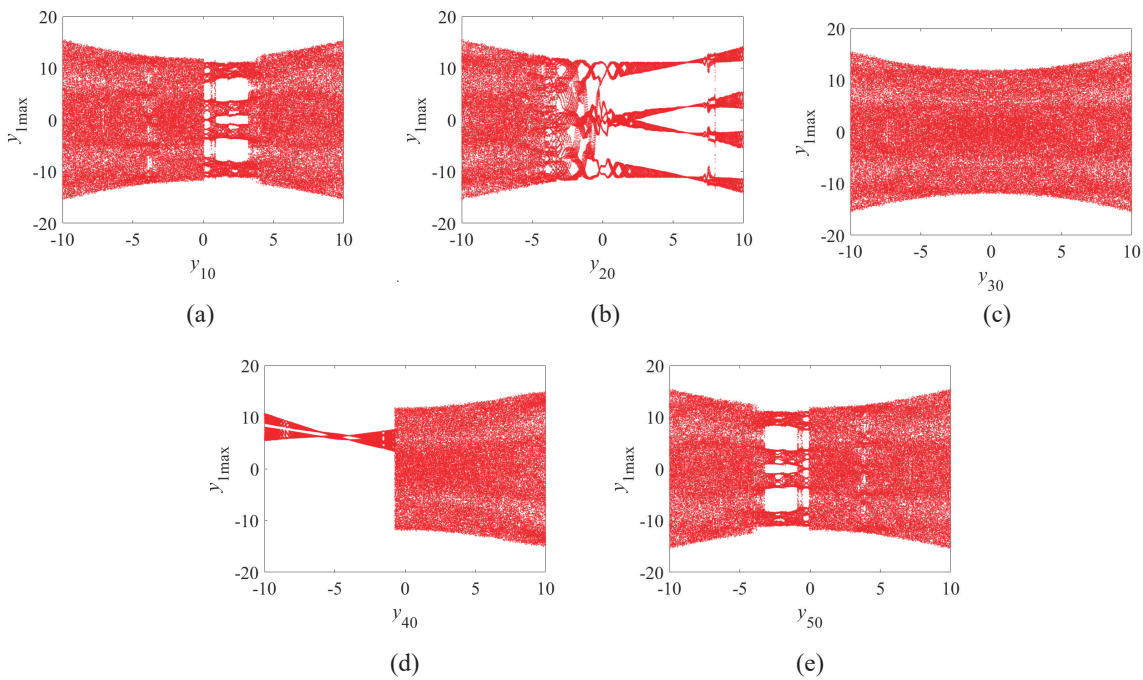

Fig. 9 The bifurcation diagram of system HCCSs-3.1 when the initial value changes. **a** $y_{10} \in [-10, 10]$; **b** $y_{20} \in [-10, 10]$; **c** $y_{30} \in [-10, 10]$; **d** $y_{40} \in [-10, 10]$; **e** $y_{50} \in [-10, 10]$.

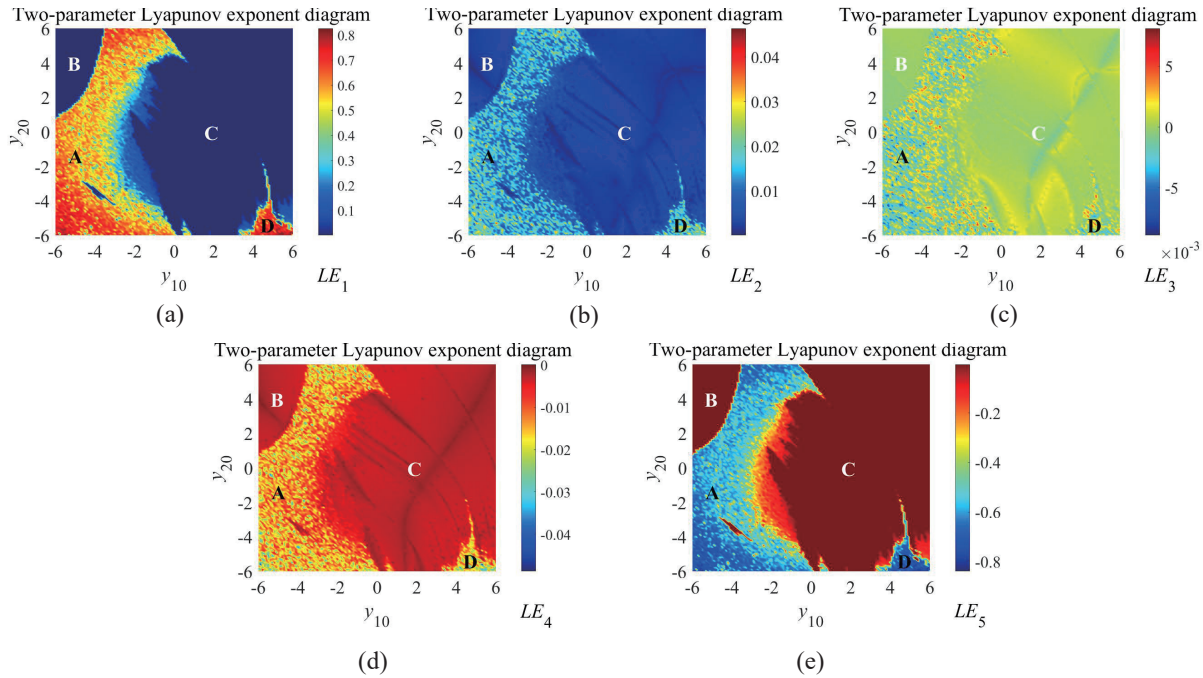

Fig. 10 Two-parameter Lyapunov exponent spectrum. **a** LE_1; **b** LE_2; **c** LE_3; **d** LE_4 ; **e** LE_5

When a changes, the system state is changeable. At $a \in (0, 1.99] \cup [2.02, 2.32] \cup [2.43, 2.44] \cup [2.49, 2.51] \cup [3.07, 3.1] \cup [3.15, 3.16]$, the five Lyapunov exponents of system HCCSs-3.1 are approximately zero, which indicates that HCCSs-3.1 is periodic or quasi-periodic. In other regions, system HCCSs-3.1 is chaotic or hyperchaotic. In Fig. 8, the phase trajectories on the $y_1 - y_2$ plane for different values of a are made, which can more clearly demonstrate the rich dynamic behavior of HCCSs-3.1. Several different quasi-periodic orbits can be observed in Fig. 8. Of course, in addition to the orbits displayed in Fig. 8, there are other different quasi-periodic and chaotic(hyperchaotic) orbits.

4.3 Bifurcation diagram of system HCCSs-3.1 for different initial system values

Set the system parameters to $a = 5$, and the initial values are changed using the following value sets: $(y_{10}, -6, 6, 6, 6)$, $(6, y_{20}, 6, 6, 6)$, $(6, -6, y_{30}, 6, 6)$, $(6, 6, 6, y_{40}, 6)$, and $(6, -6, 6, 6, y_{50})$, where $y_{10} \in [-10, 10]$, $y_{20} \in [-10, 10]$, $y_{30} \in [-10, 10]$, $y_{40} \in [-10, 10]$, and $y_{50} \in [-10, 10]$. Then, the bifurcation diagrams of system HCCSs-3.1 are drawn in Matlab, as shown in Fig. 9a–e.

The changes in Fig. 9 show that system HCCSs-3.1 has many different orbits. That is to say, different initial values lead to different chaotic or quasi-periodic orbits. This phenomenon indicates that chaotic (hyperchaotic) orbits coexist with quasi-periodic (periodic) orbits in the constructed HCCSs-3.1 system.

4.4 Two-parameter Lyapunov exponent spectrum

Next, for system HCCSs-3.1, parameter a and initial values are set to $a = 5$ and $(y_{10}, y_{20}, 6, 6, 6)$, respectively, where $y_{10} \in [-6, 6]$, $y_{20} \in [-6, 6]$.

The trend graphs of the five Lyapunov exponents denoted as LE_1–LE_5 for the set parameters' values are shown in Fig. 10. The dynamic evolution diagrams obviously show the system state and coexistence of different dynamics.

In Fig. 10, the two-parameter Lyapunov exponent diagram analysis shows that the Lyapunov exponent of system HCCSs-3.1 is symmetric about the zero axis, and different orbits can coexist at different initial values. In regions A and D, the system HCCSs3.1 is chaotic or hyperchaotic, since LE_1 is greater than zero and LE_2 is positive or equal to zero. The system HCCSs-3.1 is periodic

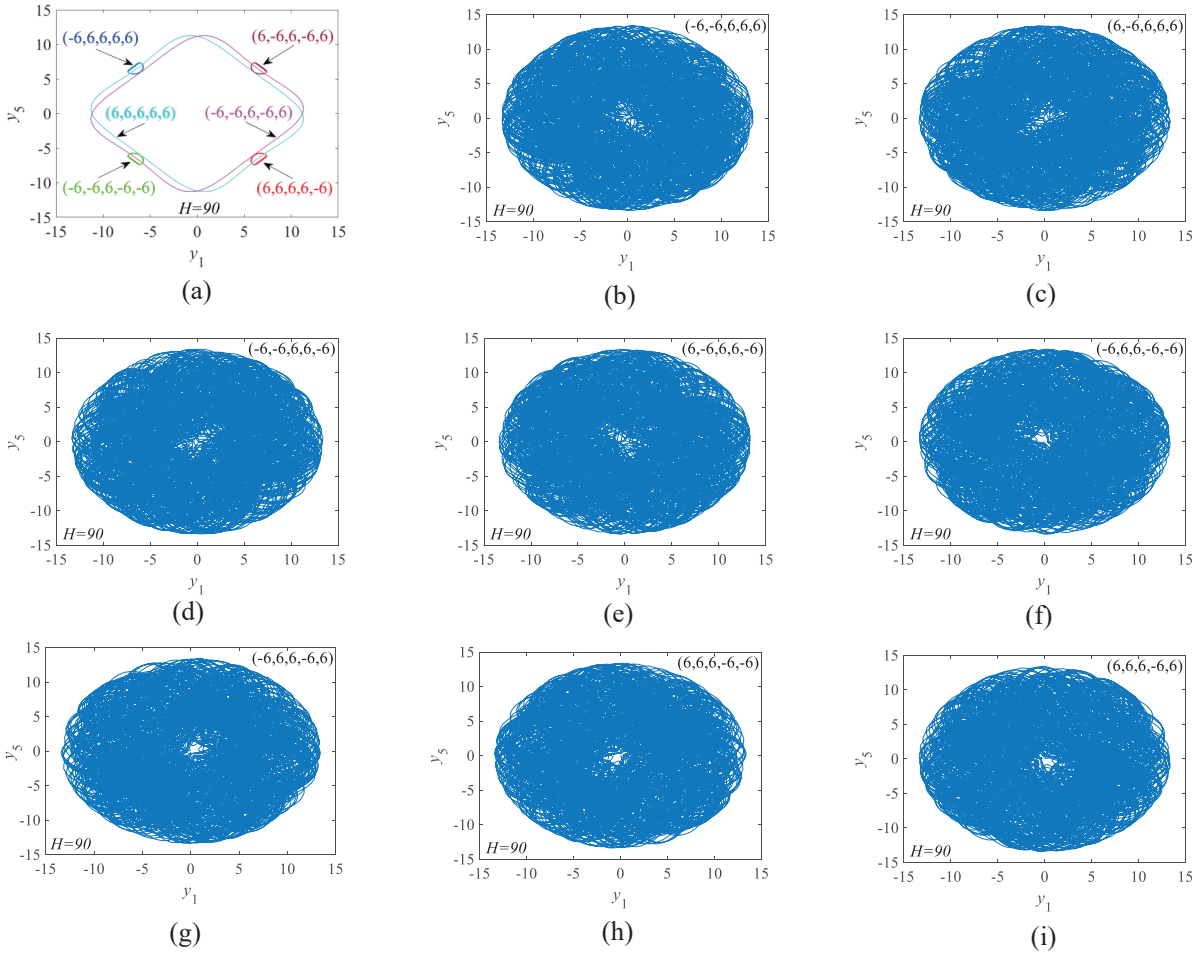

Fig. 11 Phase trajectories of equal-energy coexisting orbits in the system HCCSs-3.1. **a** Coexisting equal-energy quasi-periodic and periodic orbits; **b-e** Coexisting equal-energy and symmetric hyperchaotic orbits; **f-i** Coexisting equal-energy and symmetric hyperchaotic orbits.

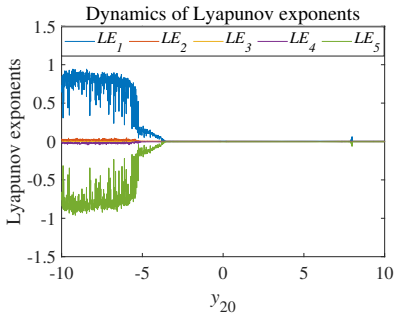

Fig. 12 Lyapunov exponent spectrum with respect to y_{20}, where $y_{20} \in [-10, 10]$

or quasi-periodic in regions B and C, because all Lyapunov exponents of system HCCSs-3.1 are approximately zero. In fact, the two-parameter Lyapunov exponent graph of the system has a good agreement with the bifurcation graph. For instance, the system state changing process when $y_{20} = -6$ and y_{10} changes between -6 and 6 is shown in Fig. 10a. Under such conditions, the system experienced the following state-changing process: chaos (hyperchaotic) $\rightarrow$ period (quasi-period) $\rightarrow$ chaos (hyperchaotic) $\rightarrow$ period (quasi-period) $\rightarrow$ chaos (hyperchaotic), which corresponds to Fig. 9a. This confirms the multistable property of system HCCSs-3.1 from another aspect. The multistability analysis of system HCCSs-3.1 is presented in Section. 4.5.

4.5 Multistability analysis

As mentioned in Section. 3.6, the multistable property of system HCCSs-3.1 is analyzed.

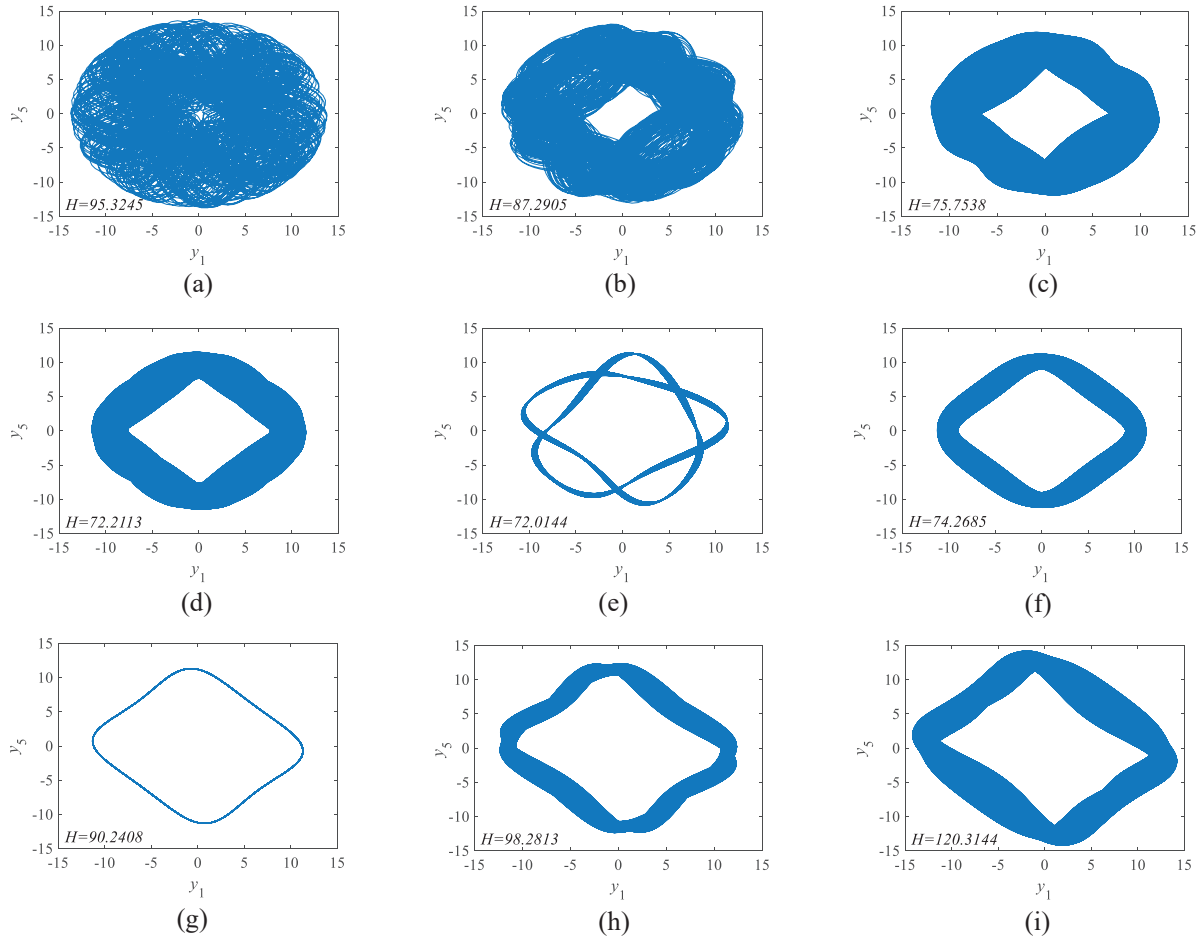

Fig. 13 Phase trajectories of the $y_1 - y_5$ plane produced by the system HCCSs-2.3 at different initial values of y_{20}. **a** $y_{20} = -6.83$; **b** $y_{20} = -5.53$; **c** $y_{20} = -2.74$; **d** $y_{20} = -0.65$; **e** $y_{20} = -0.17$; **f** $y_{20} = 2.13$; **g** $y_{20} = 6.04$; **h** $y_{20} = 7.25$; **i** $y_{20} = 9.83$.

4.5.1 Equal-energy orbit coexistence

Set the system parameter of system HCCSs-3.1 to $a = 5$ and change the sign of initial value (6, −6, 6, 6, 6) of system HCCSs-3.1. This is done to ensure that the Hamiltonian energy of the system is kept unchanged at 90, as given by (18). The initial conditions of system HCCSs-3.1 are in turn set as follows: (6, 6, 6, 6, 6), (−6, −6, 6, −6, 6), (−6, 6, 6, 6, 6), (6, 6, 6, 6, −6), (6, −6, 6, −6, 6), (−6, −6, −6, −6, −6), (6, 6, 6, −6, 6), (6, −6, 6, 6, 6), (6, −6, 6, 6, −6), (−6, −6, 6, 6, 6), (−6, −6, 6, 6, −6), (−6, 6, 6, −6, 6), (6, 6, 6, −6, 6), (−6, 6, 6, −6, −6), and (6, 6, 6, −6, −6). In this way, periodic, quasi-periodic, and hyperchaotic orbits with the same energy can coexist in system HCCSs-3.1.

There are 13 orbits with the same energy coexisting in system HCCSs-3.1, and these orbits have symmetry. The phase trajectory diagram of system HCCSs-3.1 corresponding to the initial value is shown in Fig. 11. The coexistence of two periodic orbits and four quasi-periodic orbits can be observed in Fig. 11a; Fig. 11b–e show four hyperchaotic orbits with symmetry; Fig. 11f-i show another four hyperchaotic orbits with symmetry. This shows that system HCCSs-3.1 can produce orbital coexistence with the same Hamiltonian energy. In other words, there is a multistable property of the same Hamiltonian energy.

4.5.2 Different-energy orbit coexistence

Like system HCCSs-2.3, system HCCSs-3.1 also has orbit coexistence of different Hamiltonian

energies, which indicates that this system has rich dynamic properties.

Let the system parameter be $a = 5$. Change the initial value y_{20} of the system, using (6, y_{20}, 6, 6, 6), where $y_{20} \in [-10, 10]$. Fig. 12 is the Lyapunov exponent spectrum of system HCCSs-3.1. Fig. 9b is the bifurcation diagram under the same range.

Set the initial value y_{20} of system HCCSs-3.1 to −6.83, −5.53, −2.74, −0.65, −0.17, 2.13, 6.04, 7.25, 9.83 in turn while keeping the other system parameters unchanged. Fig. 13a–i are the phase trajectories on the $y_1 - y_5$ plane. Specifically, Fig. 13a and b show hyperchaotic orbits; Fig. 13c–f, h, and i show the quasi-periodic orbits; and Fig. 13g shows a periodic orbit. It should be noted that the Hamiltonian energies of these orbits are different, and in addition to these orbits, system HCCSs-3.1 has infinitely many orbits.

5 NIST test

The National Institute of Standards and Technology (NIST) test[52] is an efficient tool for detecting random sequences, which can detect whether a data meets the requirements of a pseudo-random sequence. The NIST test has 15 test items. Each item generated a $P - value$ during the test. By judging the $P - value$ of each item, it was determined whether the sequence met the requirements or not. To meet the requirements, three necessary conditions must be met:

(1) Generally, on the basis of a significance level of $\alpha = 0.01$, the $P - value$ of each test item must be larger than or equal to α; (2) The corresponding pass ratio should be within a range that can be calculated by $\hat{p} \pm 3\sqrt{\hat{p}(1-\hat{p})/n}$, where $\hat{p} = 1-\alpha$. To test the accuracy of the results, the length of test data was selected to be 100 million bits, and data were divided into 100 groups; so, $n = 100$. Based on the given formula, the ratio of passing the test was calculated as [0.9601, 1.0298]. (3) The $P-value_T$ must be greater tha 0.0001. $P-value_T$ can be calculated by $P - value_T = igamc(\frac{9}{2}, \frac{\chi^2}{2})$, where $\chi^2 = \sum_{i=1}^{10} \frac{(F_i-(n/10))^2}{n/10}$, F_i is the 10 corresponding to each $P-values$ subinterval value, and $F_1 + F_2 + \cdots + F_{10} = n = 100$.

In the test, the parameters of system HCCSs-2.3 were set using $(a, b) = (2, 2)$, and the initial values were set to $(-6, 6, 6, -6, 6)$. The system HCCSs-3.1 had $a = 5$ and the initial values of $(6, -6, 6, 6, 6)$. The test results are displayed in Table. 5. As presented in Table. 5, all $P - value$, $P - value_T$, and Proportion could satisfy the above-mentioned conditions. In addition, a histogram was used to examine the distribution of

Table 5 The NIST test results of systems HCCSs-2.3 and HCCSs-3.1

		$P - value$		$P - value_T$		Proportion	
No.	Statistical Test	HCCSs-2.3	HCCSs-3.1	HCCSs-2.3	HCCSs-3.1	HCCSs-2.3	HCCSs-3.1
1	Frequency	0.162606	0.534146	0.2271	0.6577	0.98	1.00
2	Block Frequency	0.867692	0.437274	0.9121	0.5627	0.98	1.00
3	Cumulative Sums	0.946308	0.739918	0.9598	0.8264	1.00	1.00
4	Runs	0.534146	0.678686	0.6577	0.7805	0.99	0.99
5	Longest Run	0.474986	0.181557	0.6010	0.2537	0.98	1.00
6	Rank	0.798139	0.637119	0.8671	0.7473	1.00	1.00
7	FFT	0.455937	0.455937	0.5819	0.5819	0.99	0.99
8	Non-Overlapping Template	0.987896	0.991468	0.9862	0.9889	1.00	1.00
9	Overlapping Template	0.366918	0.075719	0.4866	0.0998	1.00	0.98
10	Universal	0.455937	0.153763	0.5819	0.2145	0.98	0.98
11	Approximate Entropy	0.191687	0.935716	0.2677	0.9535	0.99	0.99
12	Random Excursions	0.637119	0.964295	0.9776	0.9916	1.00	0.98
13	Random Excursions Variant	0.867692	0.931952	0.9941	0.9867	1.00	1.00
14	Serial	0.834308	0.137282	0.8909	0.1908	1.00	0.98
15	Linear Complexity	0.035174	0.971699	0.0403	0.9753	0.99	1.00

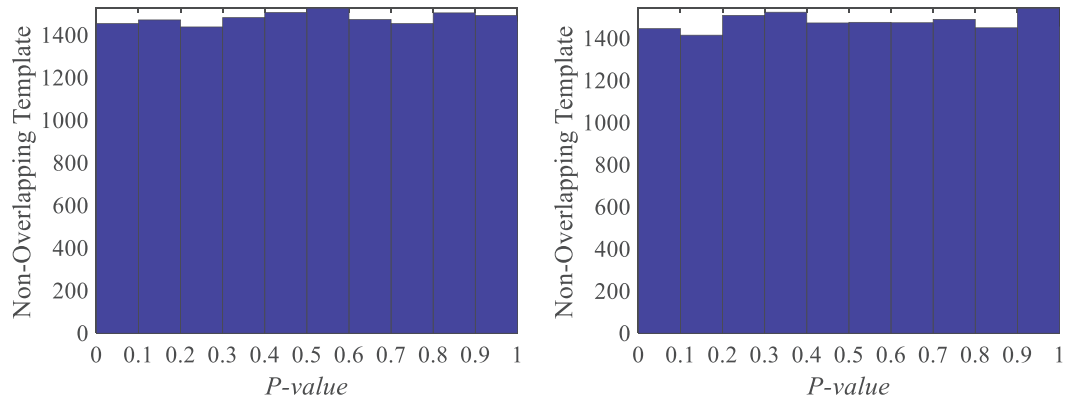

Fig. 14 The non-overlapping template $P-value$ histogram. **a** HCCSs-2.3; **b** HCCSs-3.1.

$P-values$ and observe serial uniformity. The non-overlapping items were analyzed as an example. The P-value distribution of non-overlapping templates was uniform, as shown in Fig. 14.

Thus, random sequences generated by systems HCCSs-2.3 and HCCSs-3.1 met the testing standards. Therefore, these systems could be used as pseudo-random generators.

6 Multisim circuit simulation

The simulation results obtained before this section are all based on Matlab numerical iteration, and circuit simulation is also a method to verify chaos[37, 53]. So in this section, the multistable properties of the proposed conservative system and the accuracy of numerical iteration will be further verified by designing a Multisim circuit.

It can be seen from Fig. 4 that the coexistence period and chaotic orbit of the system HCCSs-2.3 with equal energy are more recognizable, so the Multisim circuit simulation of the system HCCSs-2.3 is chosen.

Based on the system equation (11) of the system HCCSs-2.3, easy-to-implement components are selected to build the Multisim circuit of the system HCCSs-2.3. When the parameters of system HCCSs-2.3 take (a, b) = (2, 2), the designed Multisim circuit is shown in Fig. 15.

Fig. 16a-d is the circuit simulation diagram of the system HCCSs-2.3, which corresponds to the blue trace (6, 6, 6, 6, 6) in Fig. 4a, the orange trace (6, −6, 6, −6, 6) in Fig. 4b, the green trace (6, 6, 6, −6, 6) in Fig. 4c, and cyan trace (6,6,6,−6,6).

It can be seen that the results of the Multisim circuit simulation are roughly the same as the results of the Matlab numerical simulation. This further verifies the dynamic properties of the proposed system.

7 Conclusion

Based on the existing structural characteristics and construction methods of generalized Hamiltonian systems, a class of 5D conservative hyperchaotic systems with different coordinate symmetries was proposed. The proposed systems can have many types of time-reversal symmetries, up to four of them. Moreover, some systems have full time-reversal symmetry $[(y_1, y_2, y_3, y_4, y_5, t) \rightarrow (-y_1, -y_2, -y_3, -y_4, -y_5, -t)]$. The analyses of divergence, phase diagram, equilibrium point, Lyapunov exponent diagram, and bifurcation diagram have verified that the proposed system is an integer-order 5D conservative hyperchaotic system with zero divergences and zero-sum of Lyapunov exponents. This shows that the energy and volume of the proposed systems remain unchanged. In addition, the multistable phenomenon of the proposed systems is analyzed using the two-parameter Lyapunov exponent diagram and bifurcation diagram, and the analysis consequences manifest that the proposed systems have multistable features. The results demonstrate that systems of Types 2 and 3 can have finite coexisting orbits of equal energy and infinite different-energy orbits coexistence, which is verified by phase diagrams. NIST tests demonstrated that

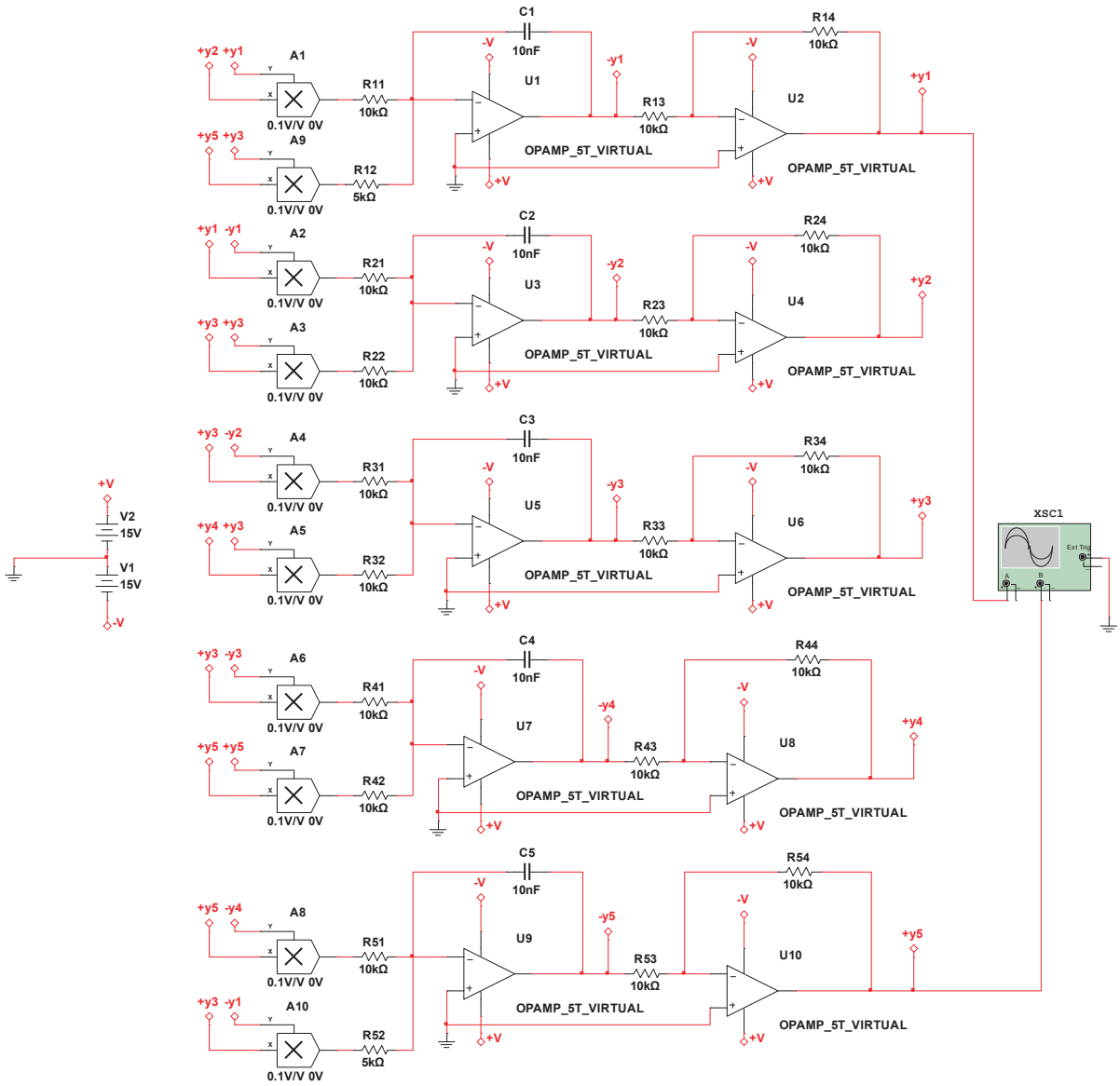

Fig. 15 Multisim circuit diagram of system HCCSs-2.3.

the proposed systems produce data with good pseudo-randomness and high complexity. Finally, the designed Multisim circuit further verifies the dynamic properties of the proposed systems.

The systems proposed in this paper possess different complex dynamic properties, such as time-reversal symmetry, wide parameter range(system HCCSs-2.3), multistability, etc. The research on time-reversal symmetry plays an important role in solving some physical problems, such as quantum mechanics. The chaotic system under the wide parameter range is more stable, the effect is better and the stability is stronger in the application. The multistability characteristics of the system can make the system show different states, and output different types of periodic and chaotic signals. This will make the system more complex and flexible, making it suitable for different application environments. And, when the system has wide parameters and multistability characteristics, its

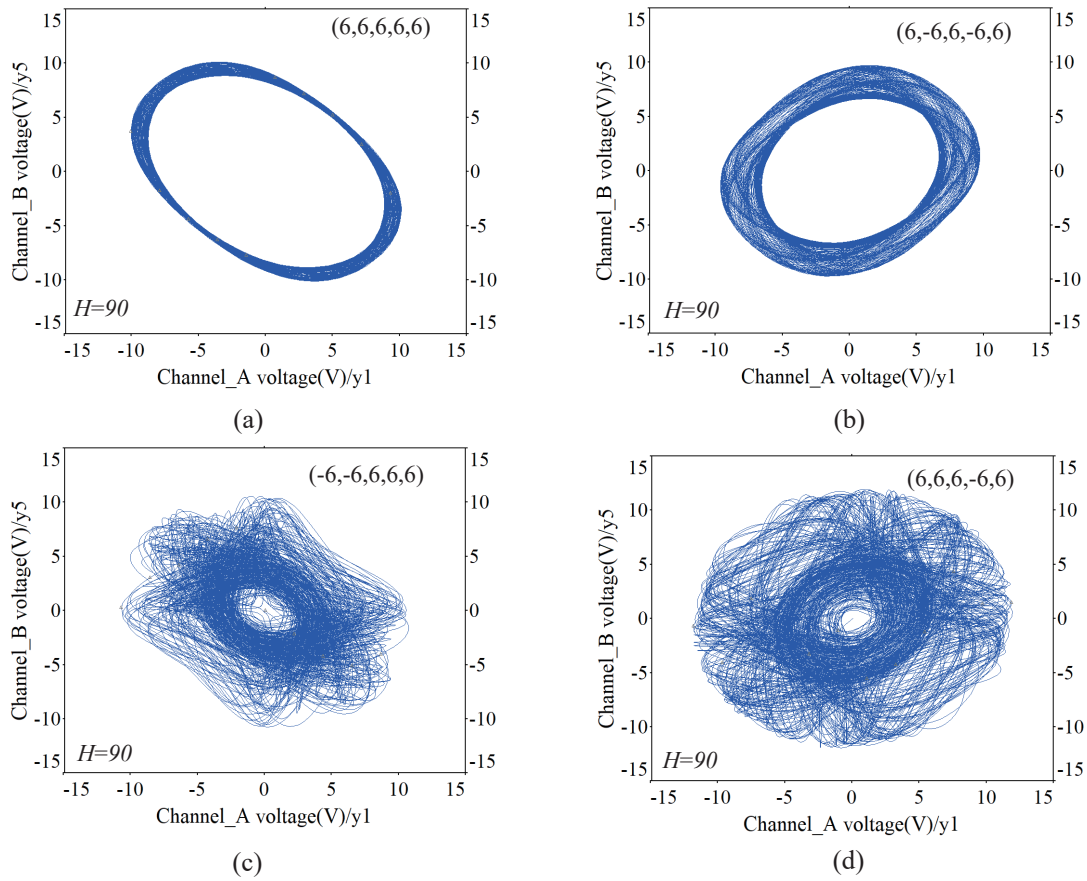

Fig. 16 The circuit simulation diagram of the system HCCSs-2.3 for different initial parametres. **a** $(6, 6, 6, 6, 6)$; **b** $(6, -6, 6, -6, 6)$; **c** $(-6, -6, 6, 6, 6)$; **d** $(6, 6, 6, -6, 6)$.

application will be more extensive. Second, the NIST test results proved the pseudo-randomness of the system from the other side, which further shows that the system can be used in image encryption, video encryption, and other encryption fields. The simulation result of the Multisim circuit verifies the dynamic characteristic of the system, and the concrete realization of its model in the future will have important value for the practical application of the system in the future.

The proposed study on multistability, related to the dynamics of multiple chaotic orbits, also constitutes a potential approach to extend the existing study of spatio-temporal brain dynamics related to brain energy, decision making processes in the brain, brain quantum processes, and consciousness [54–57]. In addition, the proposed systems have many other properties to be explored except for the multistable property and symmetry, which could be part of future work.

Acknowledgments. This work is supported by the National Key Technology R&D Program of China (No. 2018YFC0910500), the National Natural Science Foundation of China (Nos. 61425002, 61751203, 61772100, 61972266, 61802040), LiaoNing Revitalization Talents Program (No. XLYC2008017), the Innovation and Entrepreneurship Team of Dalian University (No.XQN202008), Natural Science Foundation of Liaoning Province (Nos. 2021-MS-344, 2021-KF-11-03), Scientific Research Fund of Liaoning Provincial Education Department (No. LJKZ1186), Dalian University Scientific Research Platform Program (No. 202101YB02).

Data availability. The authors declare that the data supporting the findings of this study are available within the article.

Declarations

Conflict of interest. The authors declare that we have no conflict of interests.

References

[1] Qi, G., Hu, J.: Modelling of both energy and volume conservative chaotic systems and their mechanism analyses. Commun. Nonlinear Sci. Numer. Simul. **84**, 105171 (2020)

[2] Ma, C., Mou, J., Xiong, L., Banerjee, S., Liu, T., Han, X.: Dynamical analysis of a new chaotic system: asymmetric multistability, offset boosting control and circuit realization. Nonlinear Dyn. **103**(3), 2867–2880 (2021)

[3] Jiao, X., Dong, E., Wang, Z.: Dynamic analysis and fpga implementation of a kolmogorov-like hyperchaotic system. Int. J. Bifurc. Chaos **31**(04), 2150052 (2021)

[4] Li, Y., Chen, Z., Wang, Z., Cang, S.: An effective approach for constructing a class of 4d multicluster conservative chaotic systems without external excitation. Int. J. Bifurc. Chaos **31**(13), 2150198 (2021)

[5] Qi, G., Liang, X.: Force analysis of qi chaotic system. Int. J. Bifurc. Chaos **26**(14), 1650237 (2016)

[6] Liang, X., Qi, G.: Mechanical analysis and energy cycle of chen chaotic system. Braz. J. Phys. **47**(3), 288–294 (2017)

[7] Cang, S., Wu, A., Zhang, R., Wang, Z., Chen, Z.: Conservative chaos in a class of nonconservative systems: Theoretical analysis and numerical demonstrations. Int. J. Bifurc. Chaos **28**(07), 1850087 (2018)

[8] Liang, Z., Qin, Q., Zhou, C., Wang, N., Xu, Y., Zhou, W.: Medical image encryption algorithm based on a new five-dimensional three-leaf chaotic system and genetic operation. PLoS One **16**(11), 0260014 (2021)

[9] Wu, J., Zheng, Y., Wang, B., Zhang, Q.: Enhancing physical and thermodynamic properties of dna storage sets with end-constraint. IEEE Trans. NanoBiosci. **21**(02), 184193 (2021)

[10] Zhou, S.: A real-time one-time pad dna-chaos image encryption algorithm based on multiple keys. Opt. Laser Technol. **143**, 107359 (2021)

[11] Zhang, S., Zeng, Y.: A simple jerk-like system without equilibrium: Asymmetric coexisting hidden attractors, bursting oscillation and double full feigenbaum remerging trees. Chaos Solitons Fractals **120**, 25–40 (2019)

[12] Wang, S., Wang, C., Xu, C.: An image encryption algorithm based on a hidden attractor chaos system and the knuth–durstenfeld algorithm. Opt. Lasers Eng. **128**, 105995 (2020)

[13] Gu, S., Du, B., Wan, Y.: A new four-dimensional non-hamiltonian conservative hyperchaotic system. Int. J. Bifurc. Chaos **30**(16), 2050242 (2020)

[14] Michtchenko, T.A., Vieira, R.S., Barros, D.A., Lépine, J.R.: Modelling resonances and orbital chaos in disk galaxies-application to a milky way spiral model. Astron. Astrophys. **597**, 39 (2017)

[15] Kaur, M., Singh, D., Sun, K., Rawat, U.: Color image encryption using non-dominated sorting genetic algorithm with local chaotic search based 5d chaotic map. Future. Gener. Comp. Syst. **107**, 333–350 (2020)

[16] Cao, B., Li, X., Zhang, X., Wang, B., Zhang, Q., Wei, X.: Designing uncorrelated address constrain for dna storage by dmvo algorithm. IEEE/ACM Trans. Comput. Biol. Bioinf. **19**(02), 866877 (2020)

[17] Inglada-Pérez, L., Coto-Millán, P.: A chaos analysis of the dry bulk shipping market. Mathematics **9**(17), 2065 (2021)

[18] Ubaru, S., Horesh, L., Cohen, G.: Dynamic graph and polynomial chaos based models for contact tracing data analysis and optimal testing prescription. J. Biomed. Inform. **122**,

103901 (2021)

[19] Ojoniyi, O.S., Njah, A.N.: A 5d hyperchaotic sprott b system with coexisting hidden attractors. Chaos Solitons Fractals **87**, 172–181 (2016)

[20] Li, C., Sprott, J.C., Hu, W., Xu, Y.: Infinite multistability in a self-reproducing chaotic system. Int. J. Bifurc. Chaos **27**(10), 1750160 (2017)

[21] Sprott, J.C., Jafari, S., Khalaf, A.J.M., Kapitaniak, T.: Megastability: Coexistence of a countable infinity of nested attractors in a periodically-forced oscillator with spatially-periodic damping. Eur. Phys. J. Spec. Top. **226**(9), 1979–1985 (2017)

[22] Pham, V.-T., Volos, C., Jafari, S., Kapitaniak, T.: A novel cubic–equilibrium chaotic system with coexisting hidden attractors: analysis, and circuit implementation. J. Circuit. Syst. Comp. **27**(04), 1850066 (2018)

[23] Bao, B., Bao, H., Wang, N., Chen, M., Xu, Q.: Hidden extreme multistability in memristive hyperchaotic system. Chaos Solitons Fractals **94**, 102–111 (2017)

[24] Zhang, S., Zeng, Y., Li, Z., Wang, M., Xiong, L.: Generating one to four-wing hidden attractors in a novel 4d no-equilibrium chaotic system with extreme multistability. Chaos **28**(1), 013113 (2018)

[25] Chen, M., Sun, M., Bao, B., Wu, H., Xu, Q., Wang, J.: Controlling extreme multistability of memristor emulator-based dynamical circuit in flux–charge domain. Nonlinear Dyn. **91**(2), 1395–1412 (2018)

[26] Tan, Q., Zeng, Y., Li, Z.: A simple inductor-free memristive circuit with three line equilibria. Nonlinear Dyn. **94**(3), 1585–1602 (2018)

[27] Mezatio, B.A., Motchongom, M.T., Tekam, B.R.W., Kengne, R., Tchitnga, R., Fomethe, A.: A novel memristive 6d hyperchaotic autonomous system with hidden extreme multistability. Chaos Solitons Fractals **120**, 100–115 (2019)

[28] Dong, E., Jiao, X., Du, S., Chen, Z., Qi, G.: Modeling, synchronization, and fpga implementation of hamiltonian conservative hyperchaos. Complexity **2020**, 4627597 (2020)

[29] Leng, X., Gu, S., Peng, Q., Du, B.: Study on a four-dimensional fractional-order system with dissipative and conservative properties. Chaos Solitons Fractals **150**, 111185 (2021)

[30] Rajagopal, K., Akgul, A., Pham, V.-T., Alsaadi, F.E., Nazarimehr, F., Alsaadi, F.E., Jafari, S.: Multistability and coexisting attractors in a new circulant chaotic system. Int. J. Bifurc. Chaos **29**(13), 1950174 (2019)

[31] Bao, J., Liu, Y.: Multistability and bifurcations in a 5d segmented disc dynamo with a curve of equilibria. Adv. Differ. Equ. **2019**(1), 1–15 (2019)

[32] Yu, F., Liu, L., Qian, S., Li, L., Huang, Y., Shi, C., Cai, S., Wu, X., Du, S., Wan, Q.: Chaos-based application of a novel multistable 5d memristive hyperchaotic system with coexisting multiple attractors. Complexity **2020**, 8034196 (2020)

[33] Wan, Q., Zhou, Z., Ji, W., Wang, C., Yu, F.: Dynamic analysis and circuit realization of a novel no-equilibrium 5d memristive hyperchaotic system with hidden extreme multistability. Complexity **2020**, 7106861 (2020)

[34] Yang, J., Feng, Z., Liu, Z.: A new five-dimensional hyperchaotic system with six coexisting attractors. Qual. Theory Dyn. Syst. **20**(1), 1–31 (2021)

[35] Wu, A., Cang, S., Zhang, R., Wang, Z., Chen, Z.: Hyperchaos in a conservative system with nonhyperbolic fixed points. Complexity **2018**, 9430637 (2018)

[36] Dong, E., Yuan, M., Du, S., Chen, Z.: A new class of hamiltonian conservative chaotic systems with multistability and design of pseudo-random number generator. Appl. Math. Model. **73**, 40–71 (2019)

[37] Hu, J., Qi, G., Wang, Z., Chen, G.: Rare energy-conservative attractors on global

invariant hypersurfaces and their multistability. Int. J. Bifurc. Chaos **31**(03), 2130007 (2021)

[38] Cang, S., Wu, A., Wang, Z., Chen, Z.: Four-dimensional autonomous dynamical systems with conservative flows: two-case study. Nonlinear Dyn. **89**(4), 2495–2508 (2017)

[39] Arnol'd, V.: Kolmogorov's hydrodynamic attractors. Proceedings of the Royal Society of London. Series A: Mathematical and Physical Sciences **434**(1890), 19–22 (1991)

[40] Qi, G., Zhang, J.: Energy cycle and bound of qi chaotic system. Chaos Solitons Fractals **99**, 7–15 (2017)

[41] Pasini, A., Pelino, V.: A unified view of kolmogorov and lorenz systems. Phys. Lett. A **275**(5-6), 435–446 (2000)

[42] Cheng, D., Spurgeon, S.: Stabilization of hamiltonian systems with dissipation. Int. J. Control **74**(5), 465–473 (2001)

[43] Jia, H., Shi, W., Wang, L., Qi, G.: Energy analysis of sprott-a system and generation of a new hamiltonian conservative chaotic system with coexisting hidden attractors. Chaos Solitons Fractals **133**, 109635 (2020)

[44] Zhang, Z., Huang, L.: A new 5d hamiltonian conservative hyperchaotic system with four center type equilibrium points, wide range and coexisting hyperchaotic orbits. Nonlinear Dyn. **108**(1), 637–652 (2022)

[45] Roberts, J.A., Quispel, G.: Chaos and time-reversal symmetry. order and chaos in reversible dynamical systems. Phys. Rep. **216**(2-3), 63–177 (1992)

[46] Wang, N., Zhang, G., Bao, H.: Infinitely many coexisting conservative flows in a 4d conservative system inspired by lc circuit. Nonlinear Dyn. **99**(4), 3197–3216 (2020)

[47] Lamb, J.S., Roberts, J.A.: Time-reversal symmetry in dynamical systems: a survey. Physica D **112**(1-2), 1–39 (1998)

[48] Sprott, J.C.: Symmetric time-reversible flows with a strange attractor. Int. J. Bifurc. Chaos **25**(05), 1550078 (2015)

[49] Lakshmanan, M., Rajaseekar, S.: Nonlinear Dynamics: Integrability, Chaos and Patterns. Springer, Berlin (2003)

[50] Qi, G., Hu, J., Wang, Z.: Modeling of a hamiltonian conservative chaotic system and its mechanism routes from periodic to quasiperiodic, chaos and strong chaos. Appl. Math. Model. **78**, 350–365 (2020)

[51] Qi, G., Gou, T., Hu, J., Chen, G.: Breaking of integrability and conservation leading to hamiltonian chaotic system and its energy-based coexistence analysis. Chaos **31**(1), 013101 (2021)

[52] Rukhin, A., Soto, J., Nechvatal, J., Smid, M., Barker, E.: A statistical test suite for random and pseudorandom number generators for cryptographic applications. Preprint at https://csrc.nist.gov/publications/detail/sp/800-22/rev-1a/final

[53] Wang, J., Yu, W., Wang, J., Zhao, Y., Zhang, J., Jiang, D.: A new six-dimensional hyperchaotic system and its secure communication circuit implementation. Int. J. Circ. Theor. App **47**(5), 702–717 (2019)

[54] Perlovsky, L.I., Kozma, R.: Neurodynamics of Cognition and Consciousness. Springer, Berlin, Heidelberg (2007)

[55] Freeman, W.: Neurodynamics: An Exploration in Mesoscopic Brain Dynamics. Springer, London (2012)

[56] Kasabov, N.K.: Time-space, Spiking Neural Networks and Brain-inspired Artificial Intelligence. Springer, New York (2019)

[57] Sergent, C., Corazzol, M., Labouret, G., Stockart, F., Wexler, M., King, J.-R., Meyniel, F., Pressnitzer, D.: Bifurcation in brain dynamics reveals a signature of conscious processing independent of report. Nat. Commun. **12**(1), 1–19 (2021)